Theses and Dissertations   1. Thesis and Dissertation Collection, all items

1998-12

A comparison of bulk aerodynamic methods for calculating air-sea flux

Eleuterio, Daniel Patrick.

Monterey, California. Naval Postgraduate School

http://hdl.handle.net/10945/32623

NAVAL POSTGRADUATE SCHOOL
Monterey, California

THESIS

A COMPARISON OF BULK AERODYNAMIC
METHODS FOR CALCULATING AIR-SEA
FLUX

by

Daniel Patrick Eleuterio

December 1998

Thesis Advisor: Qing Wang

Approved for public release; distribution is unlimited.

19990120 045

REPORT DOCUMENTATION PAGE

Form Approved OMB No. 0704-0188

1. AGENCY USE ONLY *(Leave blank)*	2. REPORT DATE December 1998	3. REPORT TYPE AND DATES COVERED Master's Thesis

4. TITLE AND SUBTITLE A Comparison of Bulk Aerodynamic Methods for Calculating Air-sea Flux	5. FUNDING NUMBERS
6. AUTHOR(S) Daniel Patrick Eleuterio	

7. PERFORMING ORGANIZATION NAME(S) AND ADDRESS(ES) Naval Postgraduate School Monterey CA 93943-5000	8. PERFORMING ORGANIZATION REPORT NUMBER

9. SPONSORING/MONITORING AGENCY NAME(S) AND ADDRESS(ES)	10. SPONSORING/MONITORING AGENCY REPORT NUMBER

11. SUPPLEMENTARY NOTES The views expressed in this thesis are those of the author and do not reflect the official policy or position of the Department of Defense or the U.S. Government.

12a. DISTRIBUTION/AVAILABILITY STATEMENT Approved for public release; distribution is unlimited.	12b. DISTRIBUTION CODE

13. ABSTRACT *(maximum 200 words)*

The Louis et al. (1982) bulk aerodynamic method for air-sea flux estimates is currently used in mesoscale models such as COAMPS, while the TOGA-COARE method is a state-of-the-art flux parameterization involving recent findings in surface layer meteorology, and has been proposed as a replacement to Louis. The Louis and TOGA-COARE methods were compared to direct observations during ACE-1.

Results from both methods compared well to observations for momentum flux. For sensible and latent heat flux, both methods showed good agreement in low flux regimes and underestimated the fluxes at higher values. Calculation of the transfer coefficients required to match observations indicated that the bulk transfer coefficients do not increase rapidly enough for z/L values less than -0.5. In the high wind regime, the transfer coefficients were very sensitive to static stability. The COARE method was superior to the Louis method for sensible heat flux estimates while the Louis method was better for latent heat flux. A sensitivity test was done to use the COARE roughness length parameterization in the Louis method. This resulted in slight improvement in sensible heat flux estimates for highly convective conditions. Latent heat flux was overestimated by the modified Louis parameterization in the same manner as the COARE algorithm, indicating that specification of the latent heat roughness length requires further study.

14. SUBJECT TERMS Air-sea flux, bulk parameterization, Coupled Ocean Atmosphere Mesoscale Prediction System (COAMPS), mesoscale modeling.	15. NUMBER OF PAGES 92
	16. PRICE CODE

17. SECURITY CLASSIFICATION OF REPORT Unclassified	18. SECURITY CLASSIFICATION OF THIS PAGE Unclassified	19. SECURITY CLASSIFICATION OF ABSTRACT Unclassified	20. LIMITATION OF ABSTRACT UL

A COMPARISON OF BULK AERODYNAMIC METHODS FOR CALCULATING AIR-SEA FLUX

Daniel Patrick Eleuterio
Lieutenant, United States Navy
B.A., Boston University, 1989
M.A.T., Boston University, 1990

Submitted in partial fulfillment of the requirements for the degree of

MASTER OF SCIENCE IN METEOROLOGY AND PHYSICAL OCEANOGRAPHY

from the

NAVAL POSTGRADUATE SCHOOL
December 1998

Author:
Daniel Patrick Eleuterio

Approved by:
Qing Wang, Thesis Advisor

Robert Haney, Second Reader

Carlyle Wash, Chairman
Department of Meteorology

iii

ABSTRACT

The Louis et al. (1982) bulk aerodynamic method for air-sea flux estimates is currently used in mesoscale models such as COAMPS, while the TOGA-COARE method is a state-of-the-art flux parameterization involving recent findings in surface layer meteorology, and has been proposed as a replacement to Louis. The Louis and TOGA-COARE methods were compared to direct observations during ACE-1.

Results from both methods compared well to observations for momentum flux. For sensible and latent heat flux, both methods showed good agreement in low flux regimes and underestimated the fluxes at higher values. Calculation of the transfer coefficients required to match observations indicated that the bulk transfer coefficients do not increase rapidly enough for z/L values less than -0.5. In the high wind regime, the transfer coefficients were very sensitive to static stability. The COARE method was superior to the Louis method for sensible heat flux estimates while the Louis method was better for latent heat flux. A sensitivity test was done to use the COARE roughness length parameterization in the Louis method. This resulted in slight improvement in sensible heat flux estimates for highly convective conditions. Latent heat flux was overestimated by the modified Louis parameterization in the same manner as the COARE algorithm, indicating that specification of the latent heat roughness length requires further study.

v

TABLE OF CONTENTS

ACKNOWLEDGEMENTS

I. INTRODUCTION

Surface fluxes of momentum, heat, and water vapor represent the exchange of energy and mass at the interface between the ocean and the atmosphere. These fluxes are the driving force for atmospheric and oceanic boundary layer growth, mesoscale ocean current and wave evolution, and tropical cyclone genesis and intensification. As a result, an accurate representation of these air-sea fluxes is critical to numerical prediction of a variety of weather, climate, and ocean problems. The increased interest in coupled and high resolution air-sea numerical models has resulted in a pressing need for more accurate surface flux parameterizations that are still computationally efficient. As numerical weather prediction becomes more focussed on mesoscale phenomena that are driven by the local forcing, errors in the surface fluxes result in errors in depicting the scales of interest and in capturing the evolution of the boundary layer on both sides of the interface.

Turbulent fluxes can be calculated in a variety of ways depending on the availability of the measurements. The commonly used methods include the eddy correlation method, the inertial subrange dissipation method, the flux-profile method, and the bulk aerodynamic method. Of these, only the eddy correlation method calculates the turbulent fluxes

directly using a time series of high frequency measurements of wind, temperature, and humidity (Chou, 1993). The advantages of this method is that it is direct and conceptually straight forward. Disadvantages are that expensive fast-response sensors must be used, the high-rate measurements thus obtained are not routinely available from weather stations or at-sea sources, and special platforms are required to prevent flow distortion around the sensors (Stull, 1988; Chou, 1993).

The dissipation method makes use of the spectral characteristics of the inertial subrange. For steady state turbulent flow this energy cascade produces a -5/3 slope on a log-log plot of the spectrum, from which the dissipation rate of the Turbulent Kinetic Energy (TKE) can be estimated. The frictional velocity is then obtained from the dissipation rate using Monin-Obukhov similarity theory. The major advantage of this method is that the momentum flux thus obtained is not sensitive to uncertainties associated with moving platforms such as a ship or buoy. The method is thus widely used with ship and buoy measurements. The disadvantage is that, similar to the eddy correlation method, fast-response sensors must be used to produce the appropriate time series of perturbations (Stull, 1988).

The flux-profile method uses the integrated form of the flux-profile equations based on Monin-Obukhov similarity theory and the empirical flux-profile relationships. In

general, two levels of measurements are needed, and the fluxes or scalar profiles are obtained through iteration. When only one level of measurement is available, the second level of information is obtained by parameterizing the height of the lowest altitude in the surface layer (Liu et al., 1979). The advantage of this method is that it can be applied to mean quantities from bulk measurements. The disadvantage is that it requires two levels of measurements, which are not routinely available from ships or meteorological stations.

The essence of the bulk aerodynamic method is to parameterize surface fluxes with mean quantities routinely available from conventional data sources. A variety of bulk aerodynamic schemes have been developed by different researchers for various mean environmental conditions. All of these methods are based on Monin-Obukhov similarity theory which makes use of generalized properties of the atmospheric surface layer. The fluxes are then estimated based on averaged measurements at a single level. Theoretically these are ensemble averages but more often they are space or time averages. The simplest of the bulk methods use fixed transfer coefficients based on vertical integration of empirically derived flux-profile relationships. More sophisticated models calculate the transfer coefficients as a function of static stability and wind speed. These transfer coefficients are then multiplied

3

by the wind speed profile between the ocean current and the measurement level and the moisture, temperature, or speed profile as appropriate for the flux of interest. In addition to a dependence on stability, the literature has also addressed the dependence of heat flux transfer coefficients on wind speed. Wind speed and static stability greatly affect the accuracy of these schemes since the profiles of heat, momentum and moisture are dependent on the turbulence structure. The turbulence structure is in turn dependent on the buoyancy and mechanical production in the boundary layer and in response to the large scale environmental forcing. The advantage of the bulk method is that it uses routinely available measurements of air temperature, sea surface temperature, and wind speed to estimate the fluxes and is thus the most suitable for operational numerical weather prediction. The disadvantage is that significant error can be introduced in the model in regions of complex or heterogeneous conditions or when the synoptic conditions vary largely from the conditions in which the parameterization was developed. Furthermore, the bulk aerodynamic method is by definition an estimate of the fluxes based on mean conditions which may not capture fine-scale structure significant in mesoscale models.

In numerical forecast models the consideration of accuracy with varying turbulence structure must be weighed against computational expense. In the past, the Louis

4

surface flux parameterization (Louis, 1979, Louis et al., 1982) has been widely used because it includes an assessment of stability dependence but is a non-iterative approach using an estimated bulk Richardson number to achieve closure. This results in a compact parameterization which is reasonably accurate and computationally efficient.

More recent work has established that the calculated transfer coefficients are too large in the stable case (Holtslag and Beljaars, 1989) and several modifications applying better empirical formulas for stable stratification to and to account for different roughness lengths for heat and momentum have recently been proposed (Beljaars and Holtslag, 1991; Launianen, 1995; Uno et al., 1995; and Lo, 1996). The current parameterization used in the United States Navy's operational mesoscale model, the Coupled Ocean Atmosphere Mesoscale Prediction System (COAMPS) is based on the Louis et al. (1982) method, as are several other mesoscale forecast models such as the Regional Atmospheric Modeling System (RAMS) (Pielke et al., 1992) and General Circulation models such as the BMRC AGCM (McAvaney and Hess, 1996). There have also been some studies indicating that Louis-type flux parameterizations work reasonably well in neutral and stable conditions but may break down in convective conditions (Garratt et al. 1996).

Another popular parameterization is the Liu-Katsaros-Businger (LKB) scheme (Liu et al.,1979) which uses the

roughness Reynolds number instead of the bulk Richardson number to achieve closure and uses iteration to simultaneously solve the surface layer equations based on Monin-Obukhov similarity theory. See Fairall et al. (1996b), DeCosmo et al. (1996), and Chou (1993) for discussions of this method when compared to field data and proposed modifications to improve accuracy.

In this study we will examine the modified bulk aerodynamic parameterization scheme used in the current U. S. Navy's mesoscale model (COAMPS) and compare the results to direct measurements using the eddy correlation method. The bulk parameterization, which is discussed in more detail in section II, is based on Louis (1979) but has undergone several modifications. The flux parameterization developed during the Tropical-Ocean Global Atmosphere Coupled-Ocean Atmosphere Response Experiment (TOGA-COARE) (Fairall et al., 1996b) is based on the LKB model and is specifically designed to produce more accurate flux estimates from bulk methods. This scheme will be applied to the same dataset in order to assess its skill over the Louis method as compared with direct flux measurements derived from the eddy correlation method. The TOGA-COARE algorithm is proposed as a replacement for the Louis model in COAMPS (Burk, personal communication) but the stability functions have been replaced with a polynomial fit to reduce computational expense. Despite the possible need for another correction to

roughness lengths in the wave breaking regime as discussed in DeCosmo et al.(1996), this model does allow for separate computation of the roughness lengths for heat and moisture, adjusts for skin temperature versus bucket temperature inputs to the calculation, and incorporates other improvements that are expected to produce more accurate fluxes than the original LKB scheme.

The objective of this research is to examine the accuracy of the Louis surface flux parameterization as a widely used method in current numerical weather prediction as compared to the TOGA-COARE algorithms which represent the state-of-the-art in accuracy but are more computationally expensive. Direct flux measurements calculated using the eddy correlation method are used as a benchmark. The dataset used in this study was collected during the Southern Aerosol Characterization Experiment (ACE-1) conducted in the Tasman Sea in November and December 1995 (Bates et al., 1998) and includes a variety of cases including stable and high wind situations. This database is therefore ideal for a thorough examination of surface flux parameterizations.

II. BACKGROUND

A. THE BULK AERODYNAMIC METHOD

In the surface layer, generally the lowest 10% of the boundary layer, momentum, heat, and moisture flux are nearly constant. These fluxes can be represented as:

$$\tau = \rho \sqrt{(\overline{w'u'})^2 + (\overline{w'v'})^2} = \rho u_*^2$$

$$H = -\rho C_p \overline{w'\Theta'} = -\rho c_p u_* \Theta_*$$

$$\lambda = --\rho L_v \overline{w'q'} = -\rho L_v u_* q_*$$

where τ is the wind stress, H is the sensible heat flux, λ is the latent heat flux, ρ is the air density, C_p is the isobaric specific heat, and L_v is the latent heat of vaporization. The bulk aerodynamic relationships approximating these fluxes are given in Eqs. (1)-(3):

$$\tau = \rho C_m (U - U_s)^2 \tag{1}$$

$$H = -\rho C_p C_h (U - U_s)(\theta_s - \theta) \tag{2}$$

$$\lambda = -\rho L_v C_q (U - U_s)(q_s - q). \tag{3}$$

Measured quantities are the surface (microlayer) potential temperature (θ_s) which is assumed to be in thermal equilibrium with the sea surface potential temperature (θ_s),

9

potential temperature (θ), specific humidity (q), and saturation specific humidity (q_s) as a function of sea surface temperature (SST) and sea level pressure (SLP). U_s is the current velocity. It is usually small and assumed to be zero in moderate to high wind conditions. The transfer coefficients (C_m, C_h, C_q) can be calculated based upon surface layer similarity theory. Integrating the flux-profile relationships between the respective roughness lengths (z_{0m}, z_{0h}, z_{0q}) and the measurement height z, we obtain the relationships:

$$u_* = \frac{k(U-U_s)}{\ln(z/z_{0m}) - \Psi_m(z/L) + \Psi_m(z_{0m}/L)} \tag{4}$$

$$\theta_* = \frac{k(\theta-\theta_s)}{\ln(z/z_{0h}) - \Psi_h(z/L) + \Psi_h(z_{0h}/L)} \tag{5}$$

$$q_* = \frac{k(q-q_s)}{\ln(z/z_{0q}) - \Psi_q(z/L) + \Psi_q(z_{0q}/L)} \tag{6}$$

where u_* is the friction velocity scale, θ_* is the temperature scale, q_* is the humidity scale, and k is the von Kármán constant (taken to be $k=0.4$ in Louis et al. (1982)). Ψ_m, Ψ_h, and Ψ_q are the integrated forms of the

empirical stability functions. The subscripts m, h, and q, denote the quantities for momentum, sensible heat, and latent heat respectively. L is the Monin-Obukhov length defined as:

$$L = \frac{\overline{\theta} u_*^2}{kg\theta_*}$$

(7)

where g is gravity.

The two parameterizations examined here differ in their approach to estimating the surface fluxes. The Louis method uses empirically adjusted curve fitting to approximate the stability functions and defines the appropriate scaling and stability regime by the momentum roughness length (z_{0m}), measurement height (z), and the Richardson number (R_{iB}). The TOGA-COARE algorithm calculates the roughness lengths for momentum, heat, and moisture based on the characteristics of the interfacial layer and then treats this as a second measurement level to solve iteratively for the surface layer fluxes from the flux-profile relationships.

B.   THE LOUIS PARAMETERIZATION

Following the treatment by Louis (1979), surface fluxes

11

for momentum (τ), sensible heat (H), and latent heat (λ) are given by Eqs. (1)-(3). The original development combined latent and sensible heat into a single term but these can be separated by retaining the same basic form of the equations for each parameter.

In order to get u_*, θ_*, and q_*, from measurements of the mean quantities at a single level, one must solve Eqs. (4)-(7) iteratively, particularly in unstable conditions. This process can be very computationally expensive, particularly in high resolution or large domain size models. Louis (1979) developed a more computationally efficient approach. He used the bulk Richardson number (Ri_B), given in Eq. (8) applied to a derived set of functions (F_m, F_h, and F_q) that closely match the iterative solution for the unstable case and field experiment data for the stable case. Equations (9) and (10) are the relationship between the fitted functions and the fluxes. The turbulent Prandtl number (R) in Eq. (11) is empirically derived from data collected over land. C_{mn} and C_{hn} are the momentum and heat transfer coefficients in neutral conditions.

$$R_{iB} = \frac{gz\Delta\theta}{\overline{\theta}u^2} \tag{8}$$

$$u_*^2 = a^2 u^2 F_m\left(\frac{z}{z_0}, R_{iB}\right) \tag{9}$$

12

$$u_*\theta_* = \frac{a^2}{R} u\Delta\theta F_h\left(\frac{z}{z_{0m}}, R_{iB}\right)$$

(10)

$$a^2 = \frac{k^2}{(\ln\frac{z}{z_0})^2}, \quad R = \frac{C_{hn}}{C_{mn}} \approx 0.74$$

(11)

The fitted relationship between fluxes, z_{0m}, and R_{iB} was incorporated into the global model at the European Centre for Medium-Range Weather Forecasting (ECMWF) where further modifications were made in order to obtain realistic model results. In the stable case, the fitted flux relationship was found to vanish at a critical Richardson number value of 0.21, resulting in the numerical model surface becoming energetically disconnected from the atmosphere. With no heat flux from the surface into the boundary layer, the atmosphere therefore cooled too fast. Based on approximating the analytic solution for the unstable case and field data in the stable case, Louis (1979) gives the explicit expressions of F as:

$$F = 1 - \frac{bRi_B}{1 + c|Ri_B|^{1/2}}, \quad unstable$$

(12)

13

$$F = \frac{1}{(1+b'Ri_B)^2}, \text{stable}$$

(13)

where b, b', and c are empirically derived constants.

Louis et al. (1982) modified this parameterization based on diagnostics of the global operational model at ECMWF and additional theoretical and consistency considerations. The final set of equations have the form:

$$C_m = a^2 (1 - \frac{2bRi_B}{1+2ba^2c(\frac{z}{z_o}|Ri_B|)^{1/2}}), \text{unstable}, b=5, c=7.5$$

(14)

$$C_{h,q} = a^2 (1 - \frac{2bRi_B}{1+3ba^2c(\frac{z}{z_o}|Ri_B|)^{1/2}}), \text{unstable}, b=5, c=5$$

(15)

$$C_m = a^2 (\frac{1}{1+2bRi_B(1+dRi_B)^{1/2}}), \text{stable}, b=5, d=5$$

(16)

$$C_{h,q} = a^2 (\frac{1}{1+3bRi_b(1+dRi_B)^{1/2}}), \text{stable}, b=5, d=5$$

(17)

$$k=0.4$$

(18)

where $C_{m,h,q} = a^2 F_{m,h,q}$.

There have been some modifications to the Louis et al. (1982) algorithm. Meaningful observations have never been easy to obtain in stable conditions due to lower levels of turbulence and the influence of inhomogeneities in the terrain (Garratt et al., 1996) but carefully designed experiments and more recent theory have improved the parameterization in stable boundary layers (Beljaars and Holtslag, 1991). The parameterization in COAMPS has been modified to account for different roughness lengths for heat and momentum and to use updated empirical formulations for transfer coefficients in the stable case. The momentum roughness length (z_{0m}) is estimated from the u* of the previous time step using Charnock's relation (1955), different roughness lengths for heat and momentum based on a fixed ratio of 1/10 are applied, and a modified set of empirical functions for the stable case have been substituted based on work by Holtslag and Beljaars (1989). The modified functions in the stable case are:

$$F_h = F_q = F_m = \frac{1}{1 + 10 Ri_B (1 + 8 Ri_B)} , stable$$

(19)

$$k = 0.4, \quad z_{0m} = \alpha \frac{u_*^2}{g} .$$

(20)

C. THE TOGA-COARE SURFACE FLUX ALGORITHM

The TOGA-COARE surface flux algorithm is a state-of-the-art method with the stated goal of flux accuracy of 10 W m^{-2}. The algorithm is based on the LKB method and has been modified to accommodate various difficult environmental conditions such as rough sea and the free convection limit. It also includes several physical considerations such as the cool-skin and warm-layer correction for the SST inputs and roughness length effects neglected previously because their impact individually was considered to be small.

Fairall et al. (1996b) provides a more detailed description of the algorithm which was applied to observations collected during TOGA-COARE. The algorithm calculates surface fluxes from the flux-profile relationships expressed in (4)-(6), which call for the mean quantities at two known levels. While the observations at a reference height provide the inputs at one level, the values at a second level come from the roughness height, which is defined as the lowest level in the surface layer, or alternatively the top of the interfacial sublayer. One modification in the TOGA-COARE flux algorithm to the original LKB method is the specification of the roughness length (z_{0m}). Equation (21) combines the LKB formulation for smooth flow (wind speed less than 2 m s^{-1}) with Charnock's relation, which is valid for rough flow (wind speed greater

than 8 m s^{-1}). Appropriate heat and moisture roughness lengths (z_{0h}, z_{0q}) are more uncertain. The current TOGA-COARE scheme parameterizes these roughness lengths as a function of the roughness Reynolds number (Rr) as discussed in section II.D.3. Equations (23) and (24) are the neutral transfer coefficients at the reference height in the TOGA-COARE model where R is the Prandtl number ($R= 1.0$ in Fairall, 1996b). Equation (22) gives the roughness Reynolds number (Rr) and Eqs. (25)-(28) are the empirical stability functions following Fairall et al. (1996b):

$$z_{om} = \alpha \frac{u_*^2}{g} + 0.11 \frac{\nu}{u_*}$$

(21)

$$R_r = \frac{u_* z_0}{\nu}$$

(22)

$$C_m^{1/2} = \frac{\kappa}{[\log(\frac{z}{z_{0m}}) - \psi_m(\zeta)]}$$

(23)

$$C_{h,q}^{1/2} = \frac{R\kappa}{[\log(\frac{z}{z_{0h,q}}) - \psi_{h,q}(\zeta)]}$$

(24)

17

$$\Psi_m = 2 * \ln\left[\frac{(1+X)}{2}\right] + \ln\left[\frac{(1+X^2)}{2}\right] - 2 * \arctan(X) + \frac{\pi}{2}, \, unstable$$

(25)

$$\Psi_h, \Psi_q = 2 * \ln\left[\frac{(1+Y_{h,q})}{2}\right], \, unstable$$

(26)

$$X = (1 + a_m \xi)^{1/4}, \, Y = (1 + a_{h,q} \xi)^{1/2}, \, \xi = z/L, \, a_m = a_{h,q} = 16$$

(27)

$$\Psi_{m,h,q} = -b_{m,h,q} \xi, \, stable, \, b_m = b_{h,q} = 7$$

(28)

where $\xi = z/L$ where L is the Monin-Obukhov length, defined in Eq. (7).

The TOGA-COARE parameterization is particularly concerned with accurate flux calculations for energy budget analysis in the equatorial Pacific. Therefore, another important modification to the LKB scheme is in the vertically integrated stability functions to include the free convection limit when u_* approaches zero but buoyancy flux does not. The vertical gradients of the scalar quantities are expected to show a $\xi^{-1/3}$ dependence which leads to the convective profile in Eq. (29). Equation (30) combines the standard Businger-type profiles in (25) and (26) with the free convective case in (29).

$$\Psi_c = 1.5 * \ln\left[\frac{y^2 + y + 1}{3}\right] - \sqrt{3}\arctan\left(\frac{2y+1}{\sqrt{3}}\right) + \frac{\pi}{\sqrt{3}}, \, y = \sqrt[3]{1 - \gamma \xi}, \, \gamma = 12.87$$

(29)

18

$$\Psi_{(m,h,q)} = \frac{1}{1+\xi^2}\Psi_{(m,h,q)} + \frac{\xi^2}{1+\xi^2}\Psi_c$$

<div align="right">(30)</div>

Other modifications to the LBK formulation which do not apply to this study and therefore will not be discussed in detail include a gustiness (w_g) factor which accounts for flux induced by boundary layer scale variability in calm conditions, the Webb correction ($\overline{w}$) which accounts for the requirement that mean vertical motion must occur associated with the heat flux so that net dry mass flux is zero, and the sensible heat contribution carried by precipitation (H_{sr}). The justification for these corrections is detailed

in Fairall et al. (1996b). These modifications affect the total flux estimate from the LKB formulation by about 20%. The TOGA-COARE algorithm has been verified in low wind regimes and convective conditions but may still underpredict the momentum flux in winds above 10 m s^{-1} as the LKB scheme was found to do in De Cosmo et al. (1996).

To further reduce the error in surface flux estimation, the TOGA-COARE flux algorithm includes corrections to adjust the bulk sea surface temperature (SST) to the skin temperature. These include the warm layer and cool skin effects discussed in section II.D.2.

The algorithm is applied as follows:

Step 1. Input measurement height, latitude, and

<div align="center">19</div>

longitude, water temperature sensor depth, inversion height, and surface pressure, and set all constants.

Step 2. Input measured variables: u, Θ_s, T, q, and rain rate(R). Correct Θ_s and q_s for warm layer and cool skin effects as discussed in Section II.D.2

Step 3. Assign $w_g=0.5$ m s^{-1} and neutral transfer coefficients as a first guess and compute all temperature dependent constants and initial values for u_*, T_*, and q_*.

Step 4. Modify the functions for stability by iterating Eqs. (1)-(3), (21)-(24), and (28)-(30), until convergence, which is normally within five iterations.

Step 5 & 6. Compute fluxes and wind stress, increment integrals for the warm layer correction, and go to the main loop.

D.   PHYSICAL CONSIDERATIONS

1.   Wind Speed

In the bulk parameterization scheme, the presence of wind speed denotes the role of the vertical wind shear in generating turbulent mixing and therefore turbulent fluxes. Since the parameterization is based on Monin-Obukhov similarity theory, wind conditions that violate this theory will result in problems with the bulk method. One of these

special wind regimes is in the limit of free convection when the mean wind speed is close to zero. Modifications were made in TOGA-COARE to include a gustiness wind factor in the apparent wind speed and a modified stability function to account for free convection (Fairall et al. 1996b).

High wind conditions over the ocean also can violate the assumptions of similarity theory and the bulk flux formulation. Based on observations during the Humidity Exchange Over the Sea (HEXOS) experiment, DeCosmo et al. (1996) indicates that in winds equal to or greater than 10-15 m s^{-1} flux-profile relationships for latent and sensible heat may break down. This may be due to changes in the surface layer structure due to waves, wave-breaking, and droplet evaporation. Whitecaps begin to form at winds of 3 m s^{-1} and breaking waves cover 1% of the surface at winds above 10 m s^{-1}, increasing with the cube of the wind speed. These effects may also be dependant on other variables such as wave age and direction in relation to the wind, which is not always well known. In addition to numerical modeling and synoptic models, flux parameterizations in high wind are important for better understanding and prediction of tropical cyclone genesis and intensification (see for example, Black and Holland 1995). The HEXOS observations reported in De Cosmo et al. (1996) indicated that the flux exchange coefficients do not significantly change with wind speed for water vapor flux up to speeds of 18 m s^{-1} and

sensible heat flux up to winds of 23 m s^{-1} and that the LKB scheme is valid at these speeds for heat and moisture. However, the drag coefficient and momentum roughness length were found to increase more rapidly than LKB predicts for wind speeds greater than 10 m s^{-1}. The work by Smith (1980) and DeCosmo et al. (1996) indicates that bulk transfer coefficients for heat and moisture flux are not seen to change with increasing wind speed. This contradicts the results of Liu (1979) and Fairall et al. (1990) that show a decrease of the bulk transfer coefficients with increasing wind speed, however scatter in the data prevents a definitive result. As discussed in Fairall et al. (1996b) and DeCosmo et al. (1996), the data indicates a consensus error of about 30% in estimation of the bulk transfer coefficients so the issue can not be definitively resolved without more precise formulations. Since the increase in u_* with wind is not accompanied by an increase in the heat and moisture exchange coefficients, the roughness lengths for heat and moisture must decrease with wind speed, as in the LKB formulation above a u_* value of 0.2.

2.   Sea Surface Temperature

Bulk parameterizations of sensible heat flux are particularly sensitive to accurate measurements of sea surface temperature (SST). Estimates of momentum flux can also be affected by SST accuracy since a sounding is usually

not available in numerical forecast models so stability is estimated by the air-sea temperature contrast. The theoretical development requires Θ_s to be the skin potential temperature, which ideally would be the measurement of Θ_s by an infrared radiometer (Fairall et al. 1996a). This method requires careful correction for reflected atmospheric radiance and close tolerances in terms of absolute accuracy and drift. Inexpensive, accurate, and reliable instruments are not available to directly measure the surface radiance so *in situ* measurements from sensors placed in the water are often used. Another means of measuring ocean surface temperature is from satellite-derived multi-channel sea surface temperatures (MCSST). These values are appropriate for most bulk methods since they measure the average radiance in a area related to the satellite resolution, nominally 8-25 kilometers on a side for the NOAA polar orbiters (Kidder and Vonder Haar, 1995). Accuracy is on the order of 0.6 K for the operational AVHRR instrument when compared to ship observations. MCSST retrievals use regression techniques to match the raw radiances to ship and buoy observations. These observations should therefore be considered bulk temperature values and not skin temperatures.

Ship and buoy based bulk sensors placed directly in the water generally either use floating sensors at a few

centimeters depth or measure the water temperature of the ships intake at 2-10 meter depth. As discussed in Fairall et al. (1996a), to obtain the correct interfacial temperature these measurements must be corrected for the warm layer and cool skin effects. The warm layer effect refers to the result of the fact that about half the solar radiation received is absorbed by the upper meter of the ocean. This leads to substantial diurnal variation in the profile of the first few meters of ocean mixed layer (Price et al. 1986). The temperature difference between the interfacial layer and the sensor inlet can be as much as several degrees in the first meter in very light winds with strong solar radiative flux. The cool skin effect refers to the fact that because sensible heat, latent heat, and longwave radiant fluxes occur in the upper fractions of a millimeter at the surface, a floating sensor at even a few centimeters will measure a warmer temperature than is at the interface. This "cool-skin" can be as much as 0.2 to 0.5 K lower than the water a millimeter below the surface (Fairall et al. 1996a). The ocean convective effect causes the cool skin effect to reach a maximum at night and with decreasing wind speeds.

3.   Roughness Length

An implicit assumption in Louis et al. (1982) is that the roughness lengths for momentum (z_{0m}), sensible heat (z_{0h}) and latent heat (z_{0q}) are equal. This assumption has been

examined in field studies by Beljaars and Holtslag (1991) and numerical studies by van den Hurk and Holtslag (1997) and Lo (1996) which have shown this assumption is only valid in certain specialized cases and can produce significant errors in numerical models. Physically the roughness lengths correspond to the height above the surface where the assumed log profiles for the surface layer are valid. For momentum, there is a general dependence on wind speed such that the roughness length increases with increasing wind speed. Over water, the roughness elements consist of wave crests. This would seem to be easier to parameterize than inhomogeneous terrain over land, however as discussed in Fairall et al. (1996b) there are complicating factors such as changes in the wave structure in rough seas due to whitecapping and issues relating to wave age or swell direction when coming from a different direction than the surface winds. Assuming that $z_{0m}=z_{0h}$ means that no distinction is made between the surface skin temperature and the temperature at z_{0m}. Field studies have shown that these values may differ by as much as 6 K over land. This temperature difference can be related to z_{0m} and z_{0h} by the B^{-1} ratio which is given by Eq. (31). As reported in Beljaars and Holtslag (1991), B^{-1} for homogenous vegetated surfaces has been found to be about 6 which results in a $z_{0m}/z_{0h}=10$. This ratio is applied in the current version of COAMPS for over water grid points after

calculating the value of z_{0m} using Charnock's relation and the u_* from the previous time step.

$$B^{-1} = \frac{(\theta_0 - \theta_s)}{\theta_*} \approx \frac{1}{k} \ln(\frac{z_{0m}}{z_{0h}}) \tag{31}$$

Roughness lengths for momentum are usually derived from empirically derived climatological databases over land and can be calculated over water using Charnock's (1955) relation or other more recent formulations developed for light wind conditions as discussed in section II. The current TOGA-COARE parameterization uses an empirical set of equations that use the roughness Reynolds number (Rr) as input (Liu et al. 1979). These are based on laboratory measurements in wind tunnels, theoretical considerations about the interfacial sublayer, and a requirement for relatively smooth transition between rough and smooth regimes. This relationship has been validated with a few field measurements as depicted in Figs. 1 and 2 but considerable scatter still exists. The application of a constant 1/10 ratio between momentum and heat roughness lengths results in the roughness lengths for heat continuing to increase in strong wind stress regimes ($Rr >= 0.8$) in the Louis parameterization while decreasing in the TOGA-COARE method.
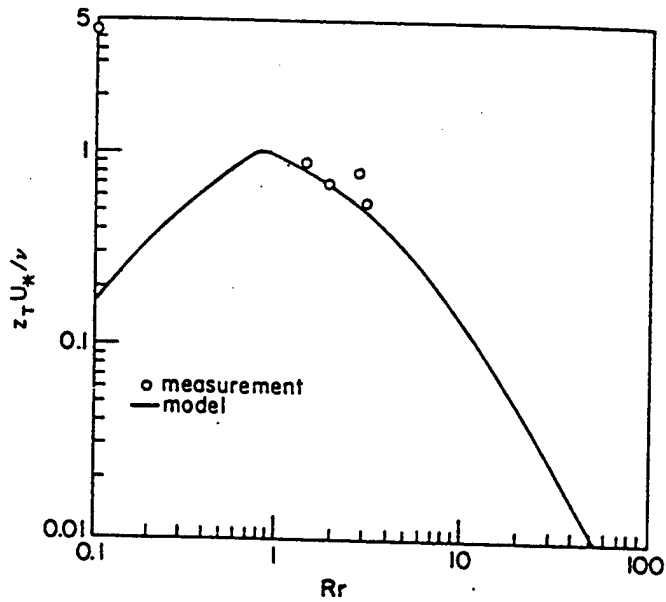
Figure 1.   Normalized sensible heat roughness length (z_T, denoted as z_{0h} in this thesis) versus roughness Reynolds number (Rr) from model (line) and field measurements (circles). From Liu et al. (1979).
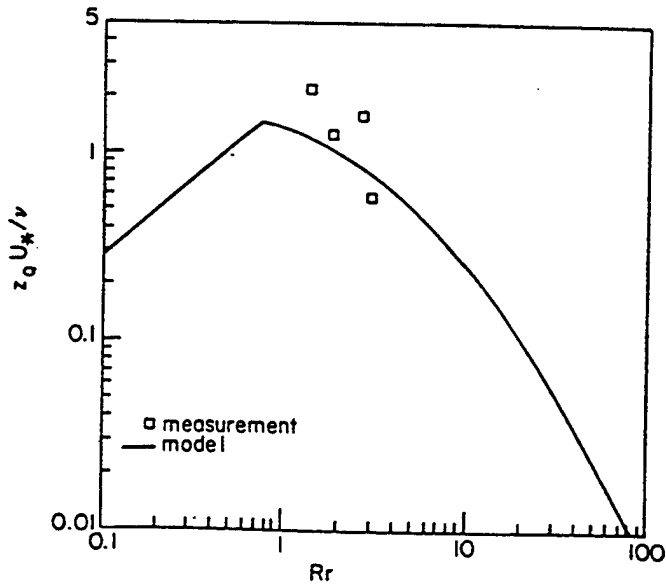

Figure 2.   Normalized latent heat roughness length (z_Q, denoted as z_{0q} in this thesis) versus roughness Reynolds number (Rr) from model (line) and field measurements (circles). From Liu et al. (1979).

27

III. METHODS

A. THE MARINE AEROSOL CHARACTERIZATION EXPERIMENT (ACE-1)

1. Overview

The Southern Hemisphere Marine Aerosol Characterization Experiment (ACE-1) was conducted from 15 November to 14 December 1995 in the South Pacific Ocean south of Tasmania. Coordinated measurements were made between the National Center for Atmospheric Research (NCAR) C-130 aircraft and a NOAA research vessel, R/V Discoverer. Details of the instrumentation and methodology are given in Wang et al. (1998a). Circular flight patterns were flown at four levels in the boundary layer and one level above. This was in order to provide longer duration at each altitude in order to improve confidence in the turbulence statistics and provide estimates of the large scale divergence from the mean wind. Some of the flights followed the southbound trajectory of tagged air columns so the flux observations crossed increasingly cold SST patterns and passed through regions of varying static stability and boundary layer structure. Winds during the observation period were moderate to strong in the 4-14 m s^{-1} range at a measurement height of 40 meters.

2. Instrumentation

Turbulence velocities were measured by the differential pressure technique using a gust probe mounted on the aircraft radome with a nominal accuracy of 0.15 m s^{-1} for vertical velocity and 1 m s^{-1} for mean winds. A Rosemount platinum fast response temperature sensor was used to measure air temperature. Water vapor was measured with a Lyman-alpha hygrometer with a specified accuracy of $\pm 4\%$ for relative humidity and corrected using a chilled mirror hygrometer. SST measurements were made with a Heimann radiometer with a manufacturer specified accuracy of + 1 °C. Shortwave radiation was measured using an Eppley PSP pyranometer and longwave radiation using an Eppley PIR pyrgeometer. See NCAR (1995) for details of the aircraft instrumentation.

B. DATA SELECTION

The data analyzed for this study were chosen based on flights with a low level leg at approximately 40 meters and a relatively straight path or gradual turning along the leg. Flights in which the low level leg was at 100 meters or above were not used due to concerns that the measurements were possibly not made in the surface layer. In general the boundary layer height was observed to be between 500 and 2000 meters during the ACE-1 period (Wang et al. 1998a). Our analysis based on Monin-Obukhov similarity theory required

measurements to remain within the surface layer, generally approximated as the lowest 10% of the boundary layer. Flights with rapid course or speed changes were discarded because platform motion can produce error in the turbulence measurements. Table 1 is a summary of the mean conditions for the selected legs based on these criteria. The low level flight legs were then segmented into 28 km sections which overlapped by half of their length in order to examine the flux and mean variables across shorter distances. Bulk input variables were then calculated as the mean value for each shorter segment. This allowed us to examine mesoscale variations in the sea surface temperature, wind speed and static stability and their effects on the flux calculations. The aircraft speed was about 110 m s^{-1} so the segments correspond to about 5 minutes of flight time.

Table 1. Flight Data Summary. MSLP is Mean Sea-Level Pressure.

Flight	Leg	Lat. (deg)	Lon. (deg)	Height (m)	MSLP (mb)	Wind Speed (m s^{-1})	Air Temp. (°C)	Sea Temp. (°C)
11	01	-53.5	137.4	40	1013	12.9	3.3	0.8
11	05	-53.2	138.6	38	1012	12.9	3.8	1.4
12	01	-48.2	137.2	39	1027	3.4	5.9	6.2
12	06	-48.5	137.6	41	1027	4.5	6.2	6.7
13	01	-49.4	138.7	44	1000	10.1	6.9	5.6
13	06	-48.4	139.1	61	1001	13.2	6.5	7.3
15	01	-47.7	145.5	39	1014	6.1	8.6	6.7
15	06	-47.1	145.8	40	1015	4.8	8.9	6.9
15	07	-46.8	144.2	39	1016	4.7	9.3	7.3
16	01	-54.1	159.0	39	995	7.3	4.2	1.7
16	04	-54.6	158.9	42	995	6.4	4.8	2.0
18	04	-45.0	144.5	39	1004	10.4	11.4	9.8
18	00	-45.2	145.4	40	1006	9.8	11.3	9.6
19	01	-46.2	148.6	37	1003	7.9	11.1	9.2
19	06	-46.8	150.9	45	1002	10.3	11.4	9.2
24	01	-45.2	143.0	41	1010	4.5	10.8	8.7
24	06	-45.2	143.9	41	1011	4.8	11.2	10.1
24	09	-45.2	144.3	42	1011	4.7	11.4	10.8
25	01	-45.9	145.7	38	1010	4.9	11.5	10.1

C.   THE EDDY CORRELATION METHOD

Turbulent fluxes were calculated directly from aircraft data sampled at high frequency using the eddy correlation method. Statistical correlation is done on the perturbations or turbulent fluctuations of vertical velocity (w'), and wind (u' or v'), heat (θ'), or moisture (q'). As reported in Wang et al (1998b), turbulence fluxes were calculated using 25 Hz data measured by a C-130 aircraft. To calculate the turbulent fluxes, cospectra of the appropriate variables are obtained using the Fast Fourier Transform (FFT) technique. The cospectra are then integrated from the smallest resolvable scale (nominally 4 meters) to 6 km. The 6 km wavelength cutoff was selected to ensure all contributions from small-scale turbulence are included without incorporating mesoscale or larger scale variations. Figure 3 is one example of the calculated cospectra.

The length of the data segments used for spectral analysis was about 5 minutes which corresponds to 28 km sub-sections of the low level flight leg. For each circular leg, the adjacent 5 minute segments overlap by half of their length. In general, turbulent fluxes were found to vary considerably along each flight leg in the ACE-1 region as demonstrated in the example in Fig. 4. This variability

justifies the sectioning of the data into smaller regions in order to analyze the impact of the highly variable environmental conditions. Overlapping the segments and treating each subset as an independent datum produces a smoother transition for analysis and is appropriate for comparison to bulk values derived from the same process of overlapping sections. The corrected pressure altitude was about 40 meters for all flights and was considered to be in the surface layer. The boundary layer was complex and varied in height from 500 to 2000 meters in the region (Wang et al. 1998b) but the assumption of surface layer constant flux is reasonable.
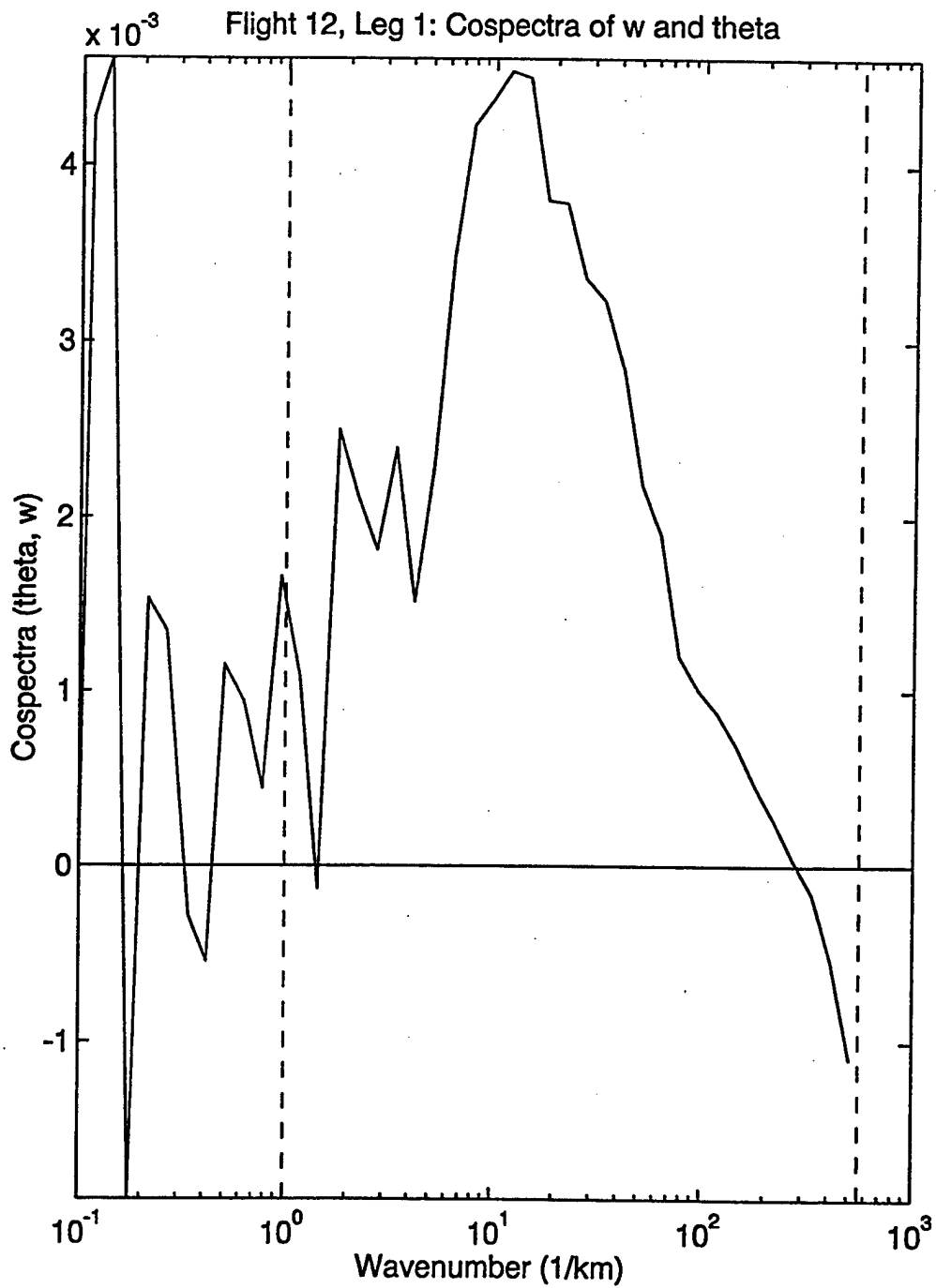
Figure 3. Sample cospectra of vertical velocity (w) and potential temperature (theta) versus wavenumber used to calculate sensible heat flux.
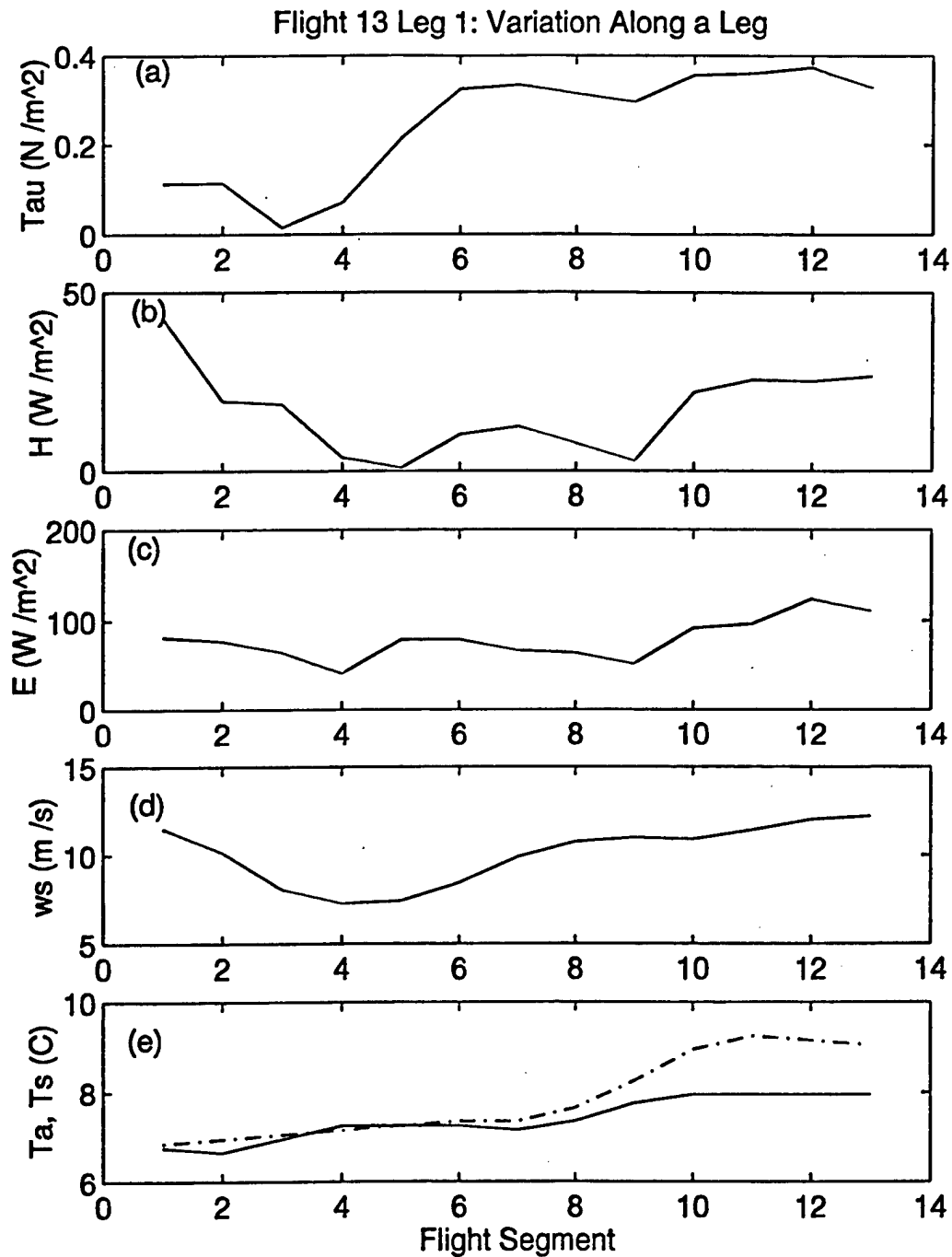
Figure 4. Example of variation in wind speed, air and sea temperature, and resultant fluxes along a circular flight leg.

D. VARIATION OF SST AND THE WARM LAYER CORRECTION

The Southern Ocean during the time and area of ACE-1 contains several strong SST fronts and includes fairly complex oceanic mesoscale features. Due to the strong sensitivity of the bulk flux methods to the accuracy of the SST, it is essential to calibrate the SST to the best available accuracy. Initial comparison of the data with satellite-derived SST values indicated a possible systematic error in the aircraft data. One of the important tasks of this research study was therefore to obtain adequate corrections to the aircraft measured skin temperatures using all available measurements and analyses.

In addition to the aircraft radiometric data, other sources of SST measurements in the ACE-1 region were satellite retrievals of Multi-Channel Sea Surface Temperatures (MCSST) from the NOAA-12 polar orbiter, conductivity/ temperature/ depth (CTD) casts by the R/V Southern Surveyor and the R/V Discoverer, and bulk inlet temperature measurements at a depth of 5 m from the R/V Discoverer. MCSST data provides the widest spatial and temporal coverage and is available for several of the flights used in this study. Figure 5 is a composite image of the satellite measured SST in the ACE-1 region. Since many of the features are masked by cloud cover at various times and the overall pattern changes very slowly, compositing the data collected during successive passes from 24 November to

37

8 December allows the major features to be seen. The strong spatial variation of SST is clearly depicted and the locations of the flights analyzed in this study are indicated by the text markers starting with "RF" and followed by the flight number. For the purpose of comparing satellite and aircraft SST measurements, precisely matching the location of the satellite data with the aircraft is not possible since the satellite data is an average temperature for a region several kilometers wide and the passes of the polar orbiter are several hours off from most of the low level flights. The CTD data has the best absolute accuracy and is closer to the surface than the inlet temperature. The CTD values may still not be exactly representative of the skin temperature due to the cool skin effect; however, the difference from the skin temperature is limited to a few tenths of a degree. The major disadvantage of the CTD data is that it was not collocated with the aircraft passes so exact comparisons were not possible. Inlet temperatures from the R/V Discoverer were recorded along the ship track every 30 minutes. These values were measured with a thermistor with a manufactured specified accuracy of 0.001 °C. The ship track overlapped the aircraft flight path on two occasions which makes direct comparisons between the platforms possible.

The basic SST measurements used in this study were the C-130 radiometric skin temperatures since the aircraft data

provides variations along the flight track along which the surface flux parameterizations were examined in segments. Table 2 is a summary of the raw measurements from the various SST data sources. The satellite retrievals in Table 2 were based on single satellite passes closest in time to the flight being analyzed and not on the 15 day average in Fig. 5. As indicated, the aircraft data consistently underestimates the surface temperature as compared to the satellite retrieved SST and ship inlet temperatures. This offset was corrected by closer analysis of the various data sources in order to approximate a constant correction factor to the C-130 data. The assumption here is that the offset in the C-130 data is constant for each flight. This appears to be reasonable since the variation in SST as depicted by the aircraft radiometer corresponds well with the variation in surface sensible heat flux calculated directly using the eddy correlation method.

Due to the strong spatial variability of SST in the ACE-1 region, the ship inlet data should be ideal to calibrate the drift in the C-130 radiometric data in regions where the two platforms overlapped. This correction was done in Wang et al. (1998b) for the Lagrangian flights when the C-130 tracked one air column for two to three days. The R/V Discoverer and C-130 tracks were compared for the entire ACE-1 period and two days were identified as having sufficient overlap. As indicated in Table 2, the ship inlet

temperature was from 1.0 to 2.2 degrees higher than the aircraft radiometric temperature. Applying a +1.2 degree correction to the input SST for the bulk method indicated that the resulting sensible heat fluxes were still systematically underestimated when compared to the directly measured sensible heat flux. Increasing the SST correction further eliminated this discrepancy in the sensible heat flux, suggesting that some of the inlet temperature measurements underestimate the skin temperature value. This discrepancy was stronger when the inlet temperatures were collected during the late afternoon and in regions with weak wind stress.

The finding that the ship inlet temperatures underestimated the skin temperature is expected. Price at al. (1986) showed considerable diurnal variation in the upper 20 meters of the ocean mixed layer. During the day, accumulation of the solar radiation in the upper mixed layer tends to form a stable warm layer in the upper few to twenty meters. If the inlet sensor is below the depth of the warm layer, the difference between the inlet temperature and the skin temperature can be significant and requires a correction.

The warm layer correction from the TOGA-COARE algorithm provides for a means to adjust bulk inlet temperatures to more closely match required surface skin temperatures. This warm layer correction subroutine is based on a simplified

form of the Price-Weller-Pinkel turbulent mixing model (Price et al., 1986). The warm layer correction is set to zero at local midnight and uses measurement time, downward solar and longwave heating, wind speed, sensor depth, and bulk water temperature to estimate the difference between the skin temperature and the temperature at measurement level. For wind speeds of 4-6 m s^{-1}, the daytime surface was found to be on the order of 0.05-1.5 K warmer than the bulk temperature at 5 m and the layer depth was on the order of 8-20 meters, with decreasing bulk-surface temperature difference and increasing layer depth values at increasing wind speeds (Fairall et al. 1996a).

The magnitude of the warm layer effect was examined using the ACE-1 data. Solar and infrared radiative flux inputs to the warm layer model were derived from aircraft measurements during flight 24 since the low level legs were in cloud free air and occurred during the main part of the local solar day. Wind stress, sensible heat and latent heat inputs were derived from aircraft data using the eddy correlation method for each flight where there was overlap between the ship and the aircraft. Similar corrections were also examined for a cloudy case by using observations from flight 12, which was in a region of moderate cloud cover.

Figures 6(a)-6(c) depict the temporal variation of the correction for three different environmental cases. Flight 24 was in clear air with low wind stress, flight 15 was in

clear air with relatively high wind stress, and flight 12 was in a cloud covered region with low wind stress. The turbulent fluxes used in the warm layer model were based on observed values for each flight. In addition to the diurnal evolution of the warm layer, the variation in the correction due to variation in the air-sea fluxes with the same diurnal heating cycle are considered and represented in each figure. The solid line represents the averaged values for the flight while the dashed lines were calculated using one positive or negative standard deviation of the observed momentum, latent heat, and sensible heat fluxes. The dashed lines therefore represent the likely upper and lower limits of the expected correction due to inhomogeneous turbulence flux in the flight region. In general, the magnitude of the correction at this latitude and season is small, on the order of 0.2 K, except in the case of very light winds at a few hours past the maximum solar heating. Despite fairly opaque cloud cover during flight 12, flights 12 and 15 were found to have fairly similar corrections under similar wind stress conditions. Insolation was reduced by about 40% during flight 12, however downwelling longwave radiation was stronger due to the emittance of the cloud layer resulting in a net heating effect on the ocean mixed layer similar to the clear air case. The warm layer effect was much larger during flight 24 with the same clear conditions. This was due to weaker turbulence mixing due to wind stress resulting

42

in a shallower layer. Because of the strong non-linear response of the warm layer model to wind stress and the high variability of wind stress along the flight legs, a hypothetical case was run using averaged latent and sensible heat fluxes and varying the wind stress by 0.01 N m^{-2} increments. As can be seen in Fig. 6(d), the warm layer effect increased dramatically for wind stresses below 0.02 N m^{-2}, which is equivalent to wind speeds on the order of 4 m s^{-1}.

The maximum warm layer correction depicted in Fig. 6(d) varied from 0.3-1.3 K due to different magnitudes of the specified wind stress. The warm layer corrections listed in Table 2 for flights 15 and 24 are based on the local solar time of the shipboard observations and the mean wind stress for the segments of the flight leg near the ship location. These values should be used with caution due to uncertainty arising from the inhomogeneity of the turbulent fluxes and the temporal evolution at the shipboard measurement location.

Based on several independent sources of SST data discussed above and the observed linear offset in the sensible heat flux values between the bulk methods and the eddy correlation data, a correction of +3.2 °C was applied to the C-130 measured SST for flight 11 and a correction of +2.2 °C was applied to flights 12-25.
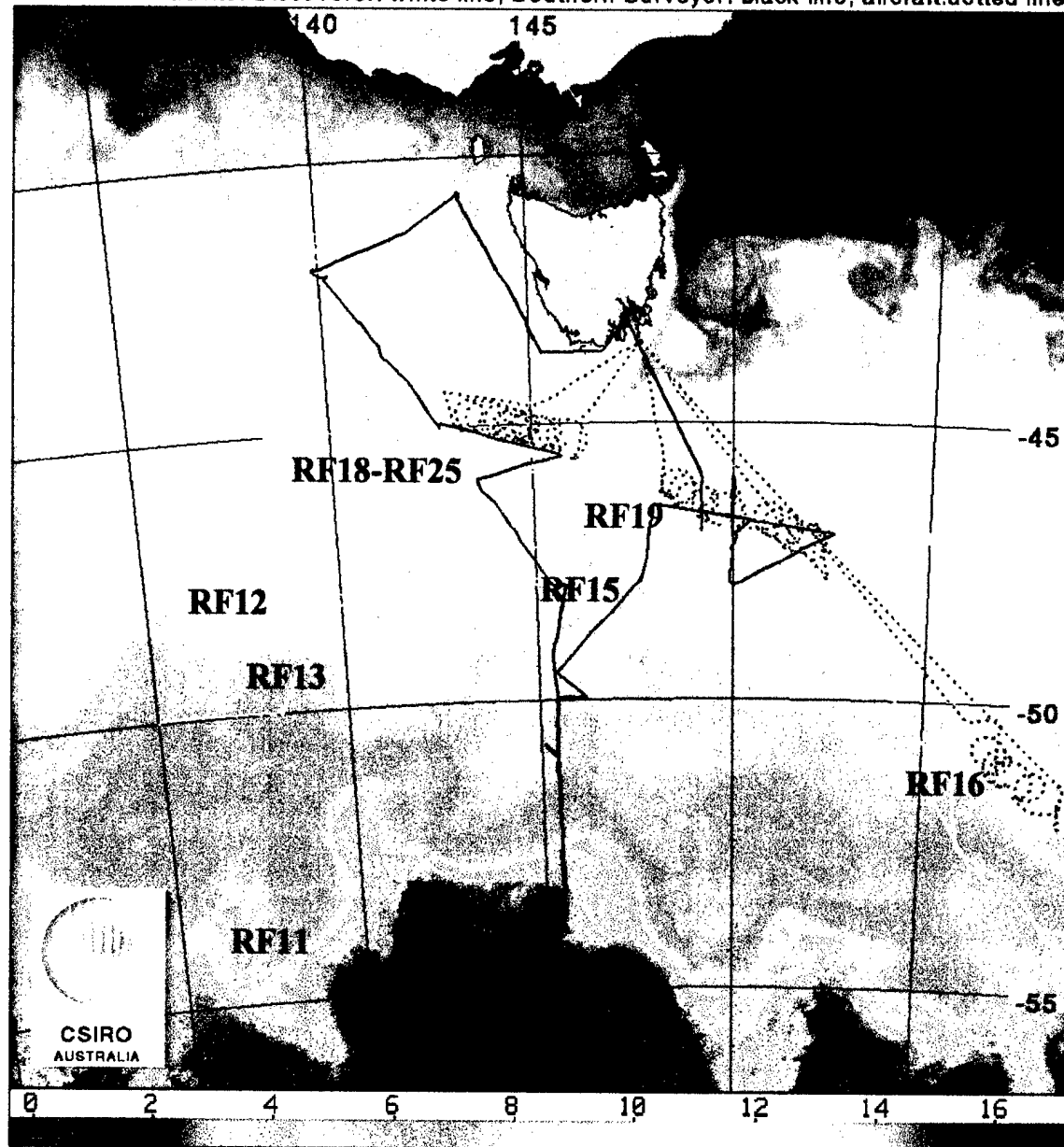
Figure 5. Composite MCSST imagery of the mesoscale oceanic variability during ACE-1. Adapted from Griffiths et. al (1998).
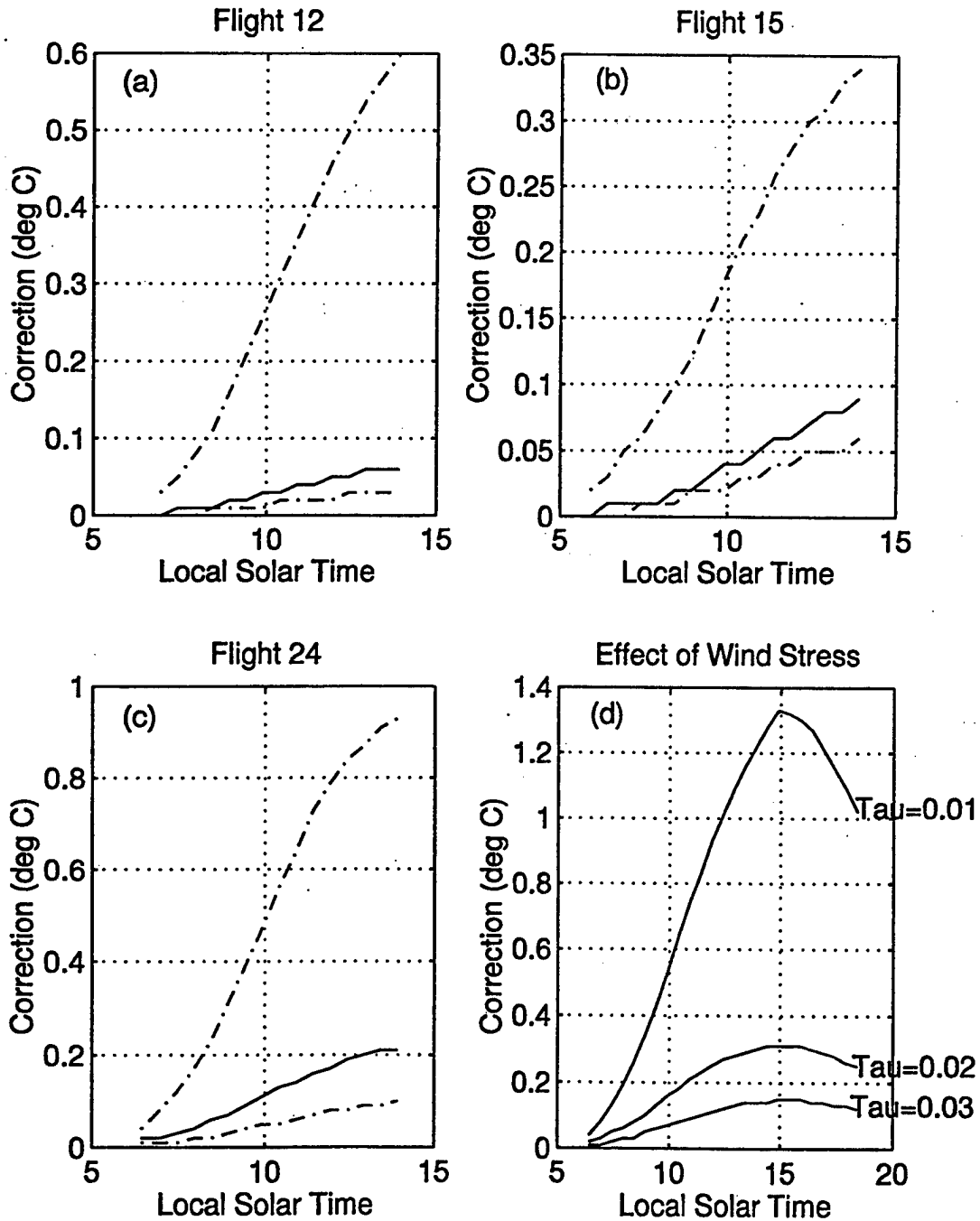
44

Figure 6. Warm layer correction for (a) flight 12 when
insolation is reduced by cloud cover in region with weak
wind stress, (b) flight 15 with full insolation and high
wind stress, (c) flight 24 with full insolation and low wind
stress, and (d) as a function of wind stress and mean latent
and sensible heat fluxes. Solid line represents mean values
and dashes represent upper and lower limits based on one
standard deviation in measured surface fluxes.

E.   THE BULK FLUX CALCULATIONS

The high-rate data collected from the C-130 was reduced
to 1 Hz data by averaging the values for each second. The
low rate data for the overlapping 28 km segments of the low
level flight legs was then averaged and these values were
used as input to the bulk methods. The calculated fluxes are
output at measurement level which is 40-60 meters. Transfer
functions are brought down to a standard level of 10 meters
and neutral conditions for comparison purposes.

Table 2. Sea Surface Temperature (°C) from various platforms and
calculations.

Flight	Lat	Lon	C-130	Satellite	Ship	Warm Layer Corr.
11	-53	138	1.1	4.5	---	---
12	-48	137	6.4	8.5	---	---
13	-49	139	6.6	9.0	---	---
15	-47	146	6.8	9.5	8.8	0.1
16	-54	159	1.7	4.0	---	---
18	-45	145	9.7	12.0	---	---
19	-46	150	9.2	12.0	---	---
24	-45	143	8.7	11.0	10.9	0.4
24	-45	144	10.4	12.0	11.4	1.1
25	-46	146	10.1	12.5	---	---

IV. RESULTS

The data collected during the ACE-1 Intensive Observation Period (IOP) covers a wide range of conditions for static stability and wind speed. The highest fluxes occurred during flights 11, 12, and 13. Flights 11 and 13 are closer to neutral static stability with moderately high wind speeds while flight 12 is strongly convective with relatively light winds. Table 3 is a summary of mean conditions and air-sea fluxes for the low level legs examined. The listed fluxes are derived from the eddy correlation method and are not corrected to a standard level but should be close to the values at 10 meters since they were measured in the surface layer. The data in Table 3 is an average value for the entire 180 km leg while the data used in the scatter plots in Figs. 10-15 discussed below is segmented into overlapping 28 km lengths as described in section III.

A. TURBULENT FLUXES

Figures 7-9 depict the momentum, sensible heat, and latent heat fluxes for all flights examined. The Louis and COARE methods follow the trend of the variability in the fluxes in this region quite well but both show error in the absolute magnitude. As seen in Fig. 7, flights 11 and 13 were in regions of high wind stress. The bulk methods

47

produced the largest discrepancies of the wind stress in these flights. The COARE algorithm comes closer but fails to capture the entire range of values. Figure 8 depicts a similar trend for sensible heat flux as that seen for wind stress. Neither method captures the maximum values seen in flight 11 and 13 however the COARE method comes closer. Figure 9 is a comparison of the latent heat flux. Flight 13 again shows large fluxes that are underestimated by the bulk methods but the Louis and COARE estimates are much closer to each other than to the observed values. Moderate latent heat fluxes are common over more flights than the sensible heat and momentum fluxes. Latent heat fluxes are overestimated in flights 18, 19 and 24 by both bulk methods however the Louis method comes closer to the observed values.

The scatter plots in Figs. 10-12 are direct comparisons of the calculated turbulent fluxes against the observed values and between the two bulk estimates. As seen in Fig. 10(a), in high wind stress conditions the Louis method underestimates the stress by about 50%. The COARE method depicted in Fig. 10(b) does slightly better but still shows large errors. Comparison of the COARE and Louis estimates in Fig. 10(c) shows that they agree very closely in low stress regions and begin to differ when the momentum flux is above 0.2 N m^{-2}. This corresponds to flights 11 and 13 where mean winds were greater than 11 m s^{-1}.

As seen in Fig. 11, in high sensible heat flux

48

conditions the bulk methods underestimate the heat flux by
about 30%. The COARE method does slightly better (Fig.
11(b)), especially with fluxes above 15 W m^{-2}, and produces
larger magnitude negative fluxes in the stable regime. In
low heat flux conditions, there is considerable scatter in
the data, with COARE doing better in some cases such as
flight 19, and Louis doing better in others such as flight
15 and 16. There are not enough cases of stable static
stability in this dataset to produce a definitive answer but
the COARE estimates do seem to verify better.

In Fig. 12, the Louis method clearly does better in
estimating the latent heat flux. Again neither method
captures the high fluxes in flight 13 and latent heat flux
estimates show more scatter than wind stress or sensible
heat flux. For fluxes less than 75 W m^{-2}, the COARE method
overestimates the latent heat flux by about 30-40%.

Figures 13-15 are comparisons of the calculated fluxes
as a function of wind speed and static stability. As can be
seen in Fig. 13(a), the regions of high wind stress were
neutral to weakly convective. The results in Figs. 13-15
indicate that the turbulent flux dependence on stability can
be separated into two regimes: the high-wind regime and the
low-wind regime, although in the high-wind regime the
stability is limited to close to neutral. These results
appear to indicate that the resultant stress is a strong
function of z/L in the high-wind conditions, although more

observations are needed for a definitive conclusion. In the low-wind regime, however, the stress appears to be insensitive to variations in static stability. In Figs. 14 and 15, large fluxes of heat and moisture are seen in near neutral conditions with reduced values in moderately convective conditions and increasing values in more convective regimes. These heat fluxes can also be separated into two groups based on low and high wind conditions with the division between these two regimes nominally at 10 m s^{-1}. The high-wind regime is where the calculated and observed fluxes from the three methods differs the most. The wind stress as computed by the bulk formulae is roughly proportional to U^2, which would indicate nearly constant C_m. As seen in Fig. 13(b), this behavior is not seen in the eddy stresses which increase much faster with wind speed. Sensible heat flux appears to decrease with wind speed for speeds less than 10 m s^{-1} and then increase with wind speed above this value. Latent heat flux seems to show a similar pattern to the sensible heat flux. While considerable scatter was seen in the actual wind stress, the bulk methods correlated very closely and fit the trend of the eddy correlation data well. In Fig. 14, the sensible heat flux increased rapidly above 11 m s^{-1}, despite near neutral stability, which is the opposite of what was found in the HEXOS data (De Cosmo et al. 1996). Figure 15 shows a modest increase in latent heat flux in stronger wind conditions as

well as with strongly convective conditions in light winds.

B.   TRANSFER COEFFICIENTS

The bulk transfer coefficients at a standard height of 10 meters are depicted in Fig. 16. Due to the day-to-day variation of the environmental conditions such as static stability and wind speed, we observe large variation in the transfer coefficients from flight to flight. However, the COARE transfer coefficients do show more variability from flight to flight and within each flight than the Louis values. However, this does not necessarily suggest that the COARE method respond faster to environmental changes than the Louis method as both methods depict similar variations in flux as seen in Figs. 7-10. As expected from the scatter plots of resultant fluxes in Figs. 11 and 12, the COARE method produces higher latent and sensible heat transfer coefficients than the Louis method for most of the observed cases but over-estimates the latent heat transfer coefficient and under-estimates the sensible heat coefficients in some regimes. The bulk methods also do not capture the variability represented in the direct flux measurements. As can be seen in Figs. 17 and 18, the flux transfer coefficients are found to be a weak function of stability except in moderate to strong wind conditions, although at these wind speeds the stability is restricted to

near neutral. However, the latent and sensible heat transfer coefficients are seen to increase with increasing wind speed. The general trend of two distinct regimes for sensible and latent heat flux is represented by the eddy correlation method as well as the bulk methods. The high wind, near neutral case and the low wind, highly convective case both result in required flux transfer coefficients based on the eddy correlation method that are much higher than those produced by either bulk method. In between these two regimes the formulation by Louis matches the observations better for latent heat flux (Fig. 17(c)) while the COARE formulation matches the sensible heat flux (Fig. 17(b)) more closely. As can be seen in Fig. 17(b) and 17(c), the thermal transfer coefficients in the bulk methods do not increase rapidly enough in the highly convective regime for z/L values less than -0.5.

C. ROUGHNESS LENGTHS

Figure 19 compares the roughness lengths for momentum, heat and moisture for the Louis and COARE methods. As seen from Fig. 19(a), the Louis method calculates slightly smaller values for momentum roughness length than the COARE method. This is expected since the COARE algorithm adds an additional term from the LKB formulation for smooth flow with the difference being the greatest at low wind speeds.

For heat (Fig. 19(b)) and moisture (Fig. 19(c)) roughness lengths, the differences are much larger as expected since the Louis method uses a fixed fraction of momentum roughness length to calculate latent and sensible heat roughness lengths while the COARE algorithm uses an empirically based parameterization.

D.   DISCUSSION

It is noted in Figs. 18(b) and 18(c) that the variations of C_h and C_q with wind speed are similar to the variations of z_{0h} and z_{0q} with Reynolds roughness number (Rr) in Figs. 1 and 2. This suggests that the observed differences in the transfer coefficients and resultant fluxes may result from the different formulations of the roughness length in the two methods. The Louis parameterization was thus modified to calculate the roughness length using the COARE formulations in Eq. (21) and Figs. 1 and 2. Figure 20 is a comparison of the COARE roughness lengths with the roughness lengths calculated from this modified version of the Louis method. The modified Louis values are much closer to the COARE values and depict more variability than the original Louis values. They still do not match the COARE roughness lengths exactly because the initial value for u_* is different between the two methods but the momentum roughness length in Fig. 20(a) is much

closer at the low values where the second term from the LKB method has the most effect.

Figures 21-23 compare the resultant fluxes from the modified Louis to the COARE and eddy correlation data. The modification of momentum roughness length has little impact on wind stress estimates between the two methods for the conditions observed the ACE-1 region. As can be seen from Fig. 21(c), the wind stress from the two bulk methods matches slightly more closely at low values although the Louis method still has lower values above 0.2 N m^{-2}. For sensible heat flux (Fig. 22) the Louis method still under estimates the flux at high values. The modified sensible heat roughness lengths do cause the Louis estimates to match the COARE results more closely. Modifying the thermal roughness length does not seem to improve the observed underestimate of the Louis method for the stable conditions. For latent heat flux, the parameterization in the COARE algorithm for z_{0q} may have a significant negative impact on the COARE results. This is supported by comparing Fig. 12 with the results in Fig. 23. The Louis latent heat fluxes are very similar to the COARE results when the same formulation for z_{0q} is used. We therefore conclude that the fact that the COARE algorithm overestimates the latent heat flux is likely caused by am inappropriate moisture roughness length (z_{0q}) parameterization.

Table 3. Summary of average aircraft loaction, stability, wind conditions, and Air-Sea Fluxes. z/L is an estimate of stability based on measurement height (z) and Monin-Obukhov Length (L) as defined in Eq. (7).

Flt.	Lat. (deg)	Lon. (deg)	Wind Speed (m s^{-1})	z/L	AirT-SeaT (°C)	Tau (N m^{-2})	H (W m^{-2})	E (W m^{-2})
11	-53.4	137.8	12.9	-0.05	-0.71	0.27	13.78	56.23
12	-48.3	137.4	4.0	-3.11	-2.14	0.06	16.78	53.18
13	-48.9	138.9	11.6	-0.20	-1.40	0.30	32.56	105.59
15	-47.4	145.6	5.5	0.01	-0.18	0.05	2.33	26.82
16	-54.1	159.0	7.2	0.12	0.08	0.04	8.22	37.92
18	-45.1	145.0	10.1	-0.05	-0.40	0.13	2.07	48.09
19	-46.5	149.8	9.2	0.04	-0.04	0.10	-1.53	28.27
24	-45.2	143.7	4.6	-0.82	-0.88	0.03	2.69	21.28
25	-45.9	145.7	4.9	-0.58	-0.73	0.03	2.16	22.37
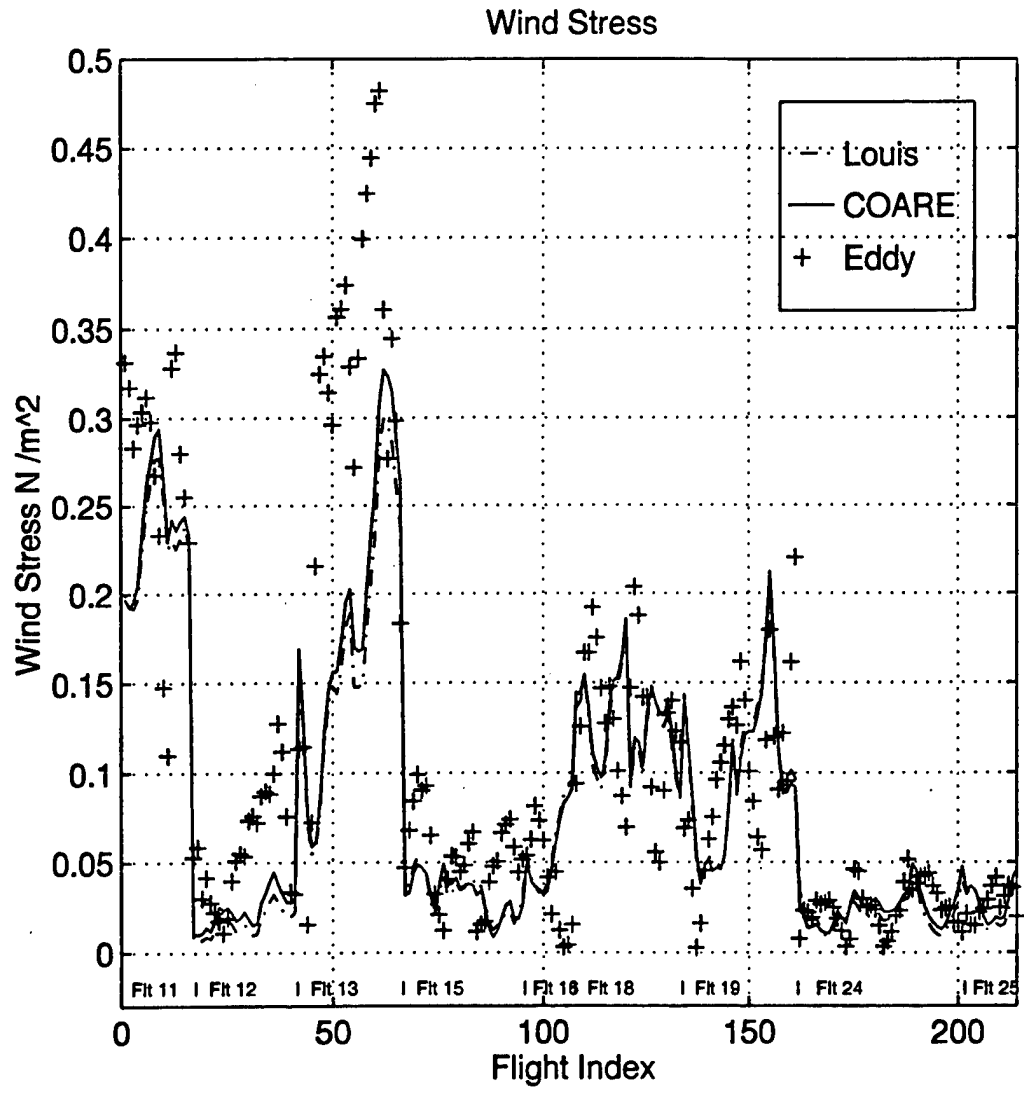
Figure 7. Calculated and observed wind stress vs. flight segment for all analyzed flights during the ACE-1 IOP.
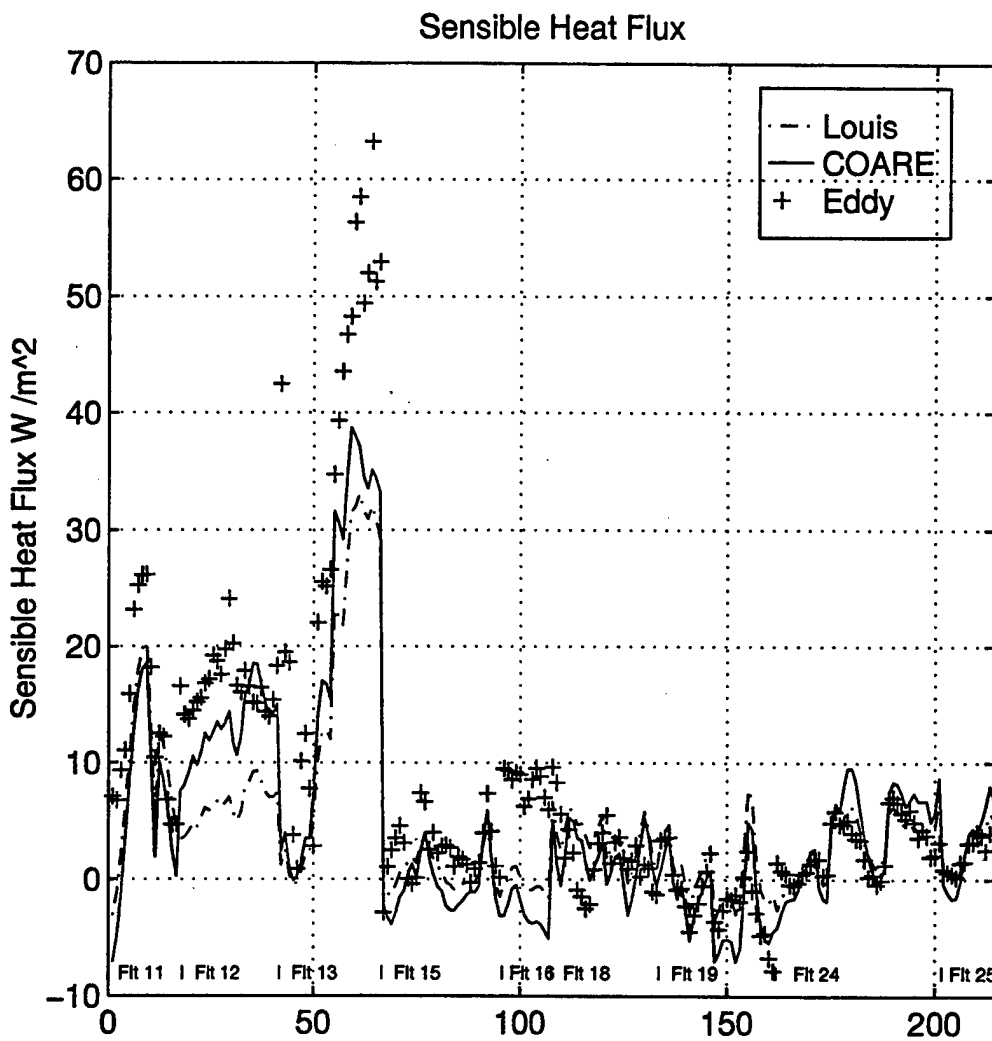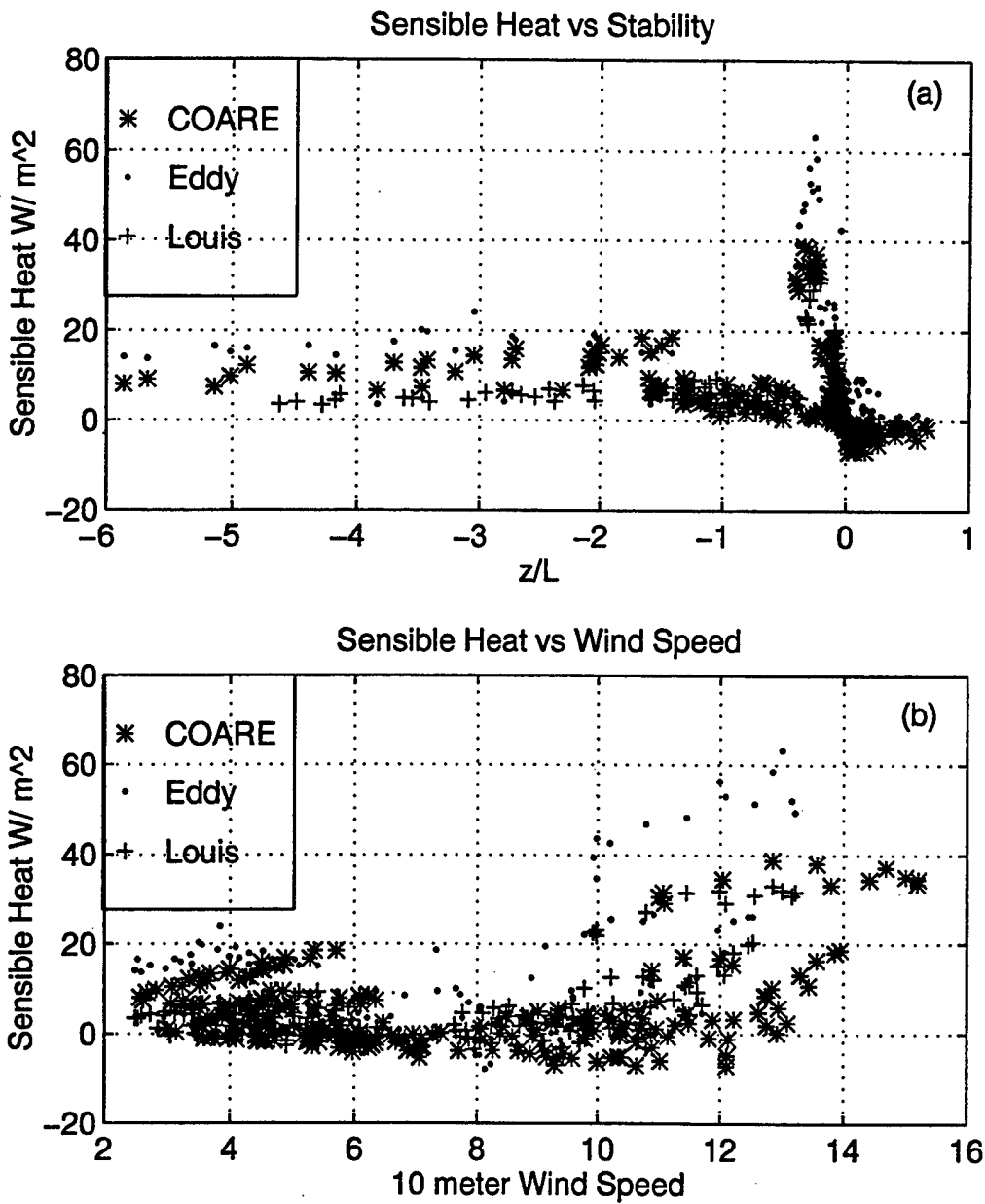
Figure 8. Same as Fig. 7, except for sensible heat flux.
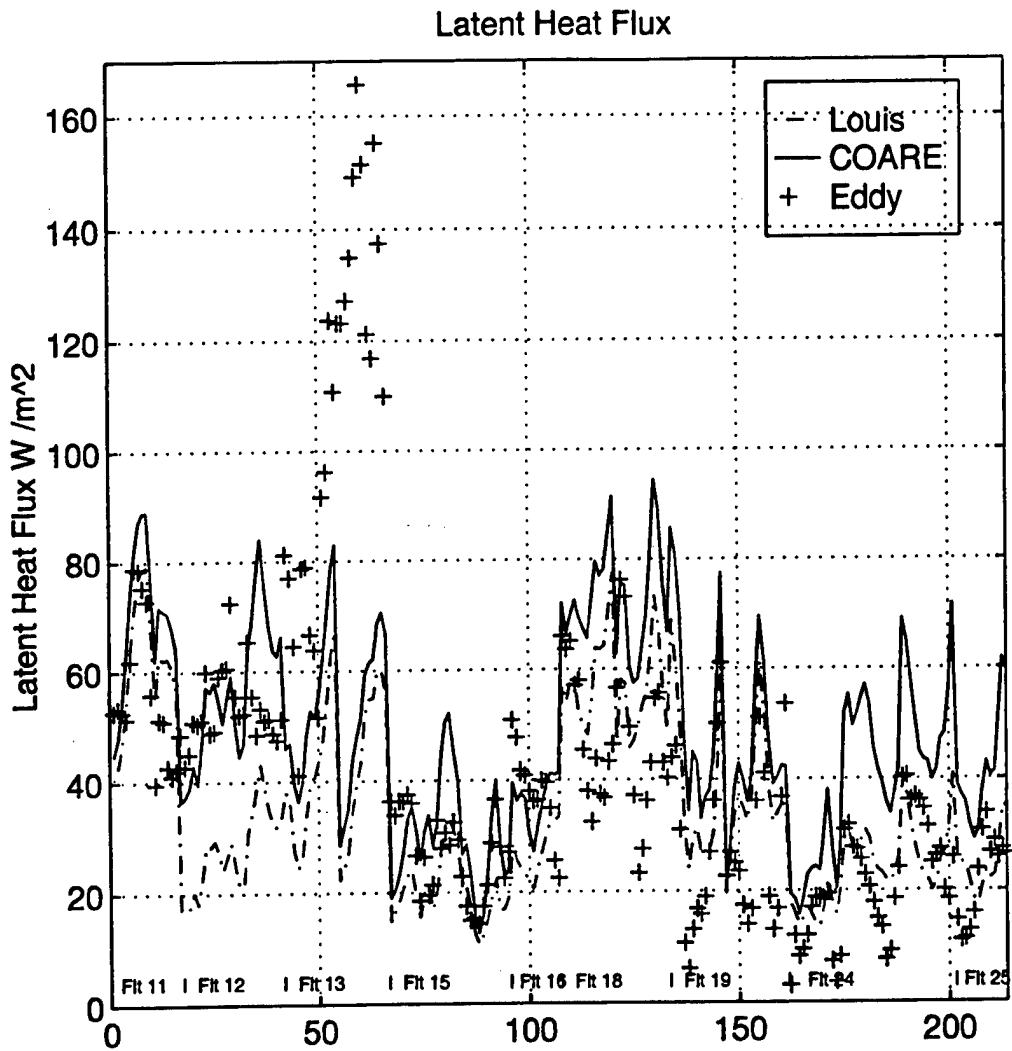
Figure 9. Same as Fig. 7, except for latent heat flux.
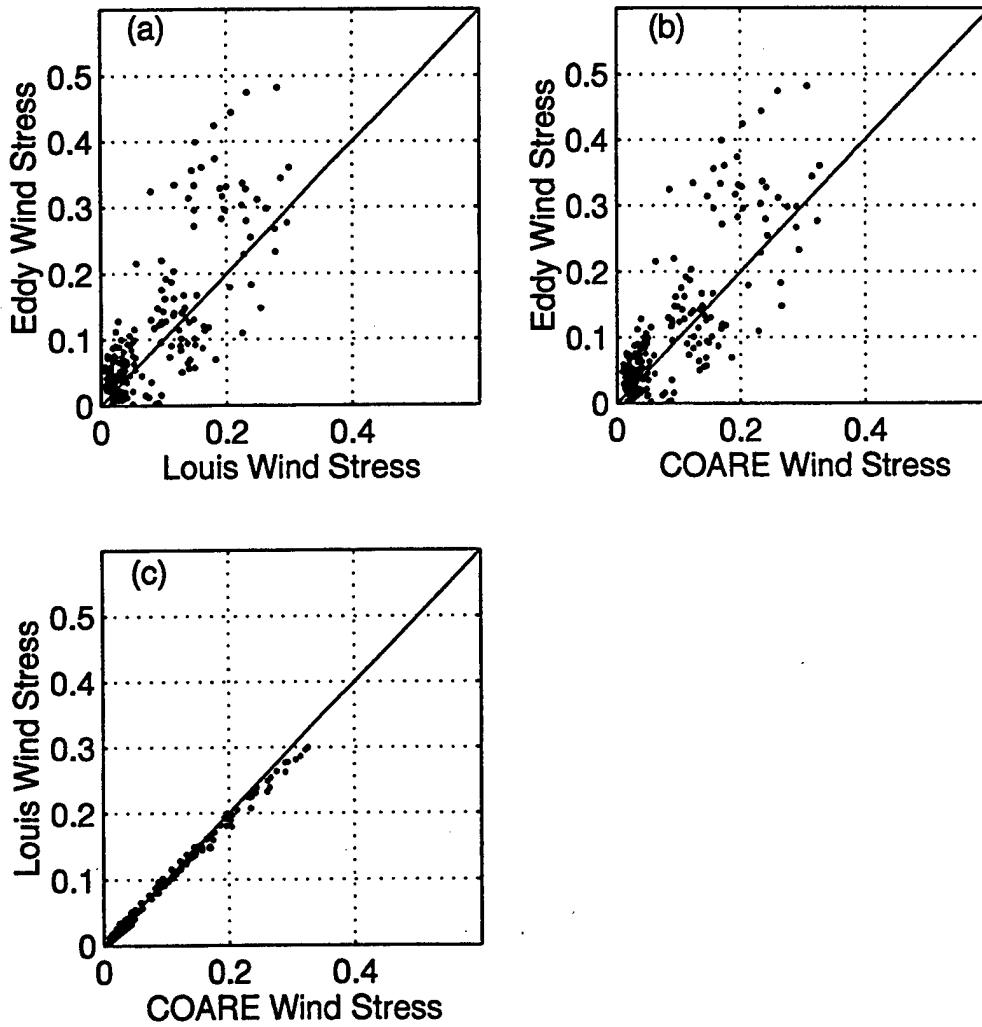
Figure 10. Comparison of the calculated wind stress (N m^{-2}) using two bulk methods and the observed flux from the eddy correlation method.
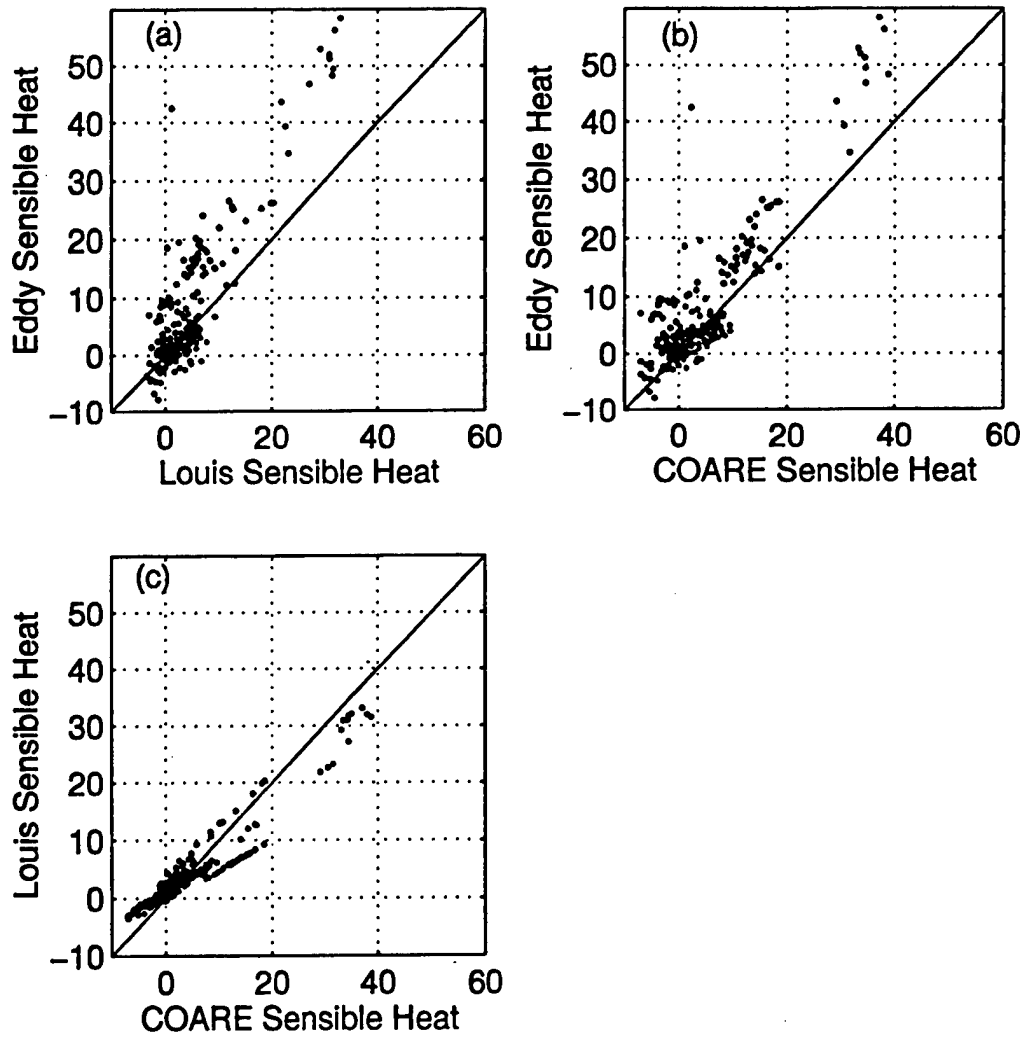
Figure 11. Same as Fig. 10, except for sensible heat flux.
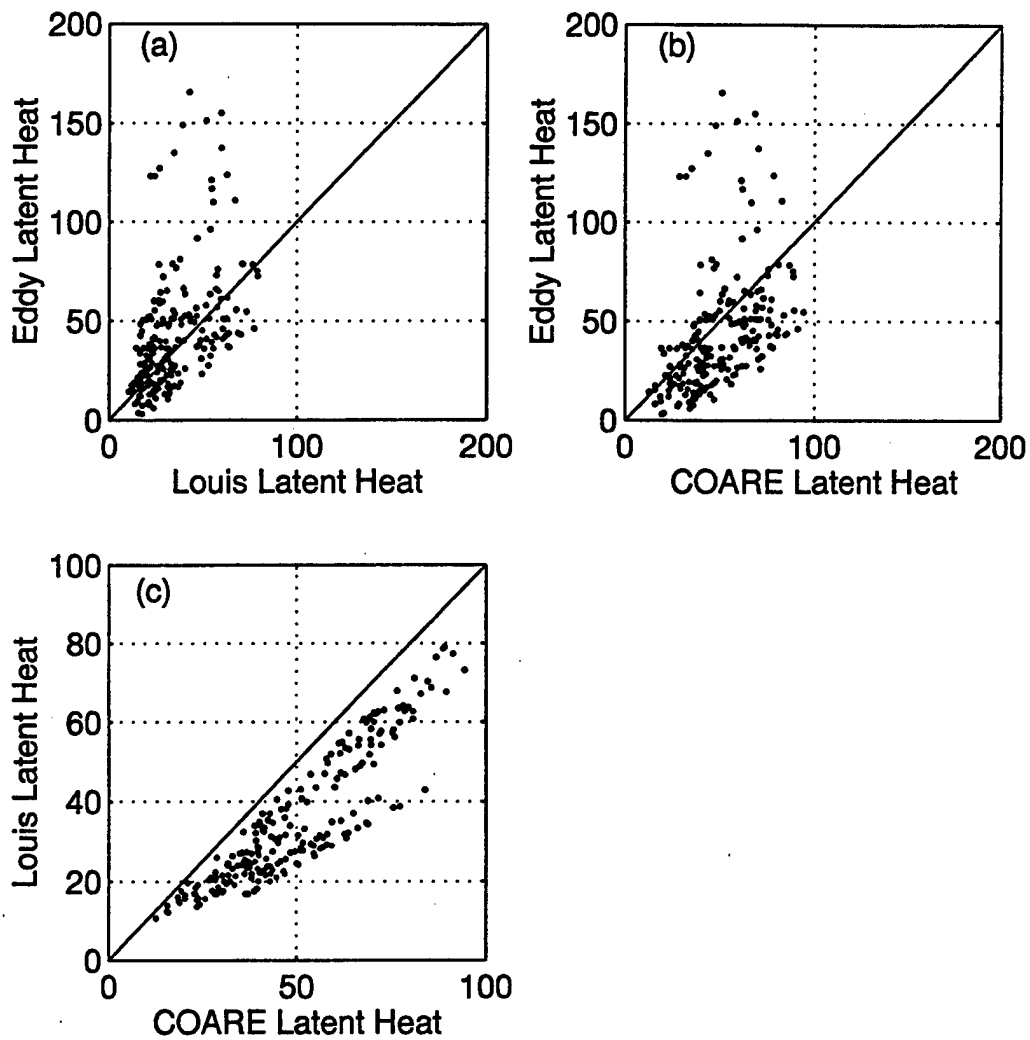
Figure 12. Same as Fig. 10, except for latent heat flux.
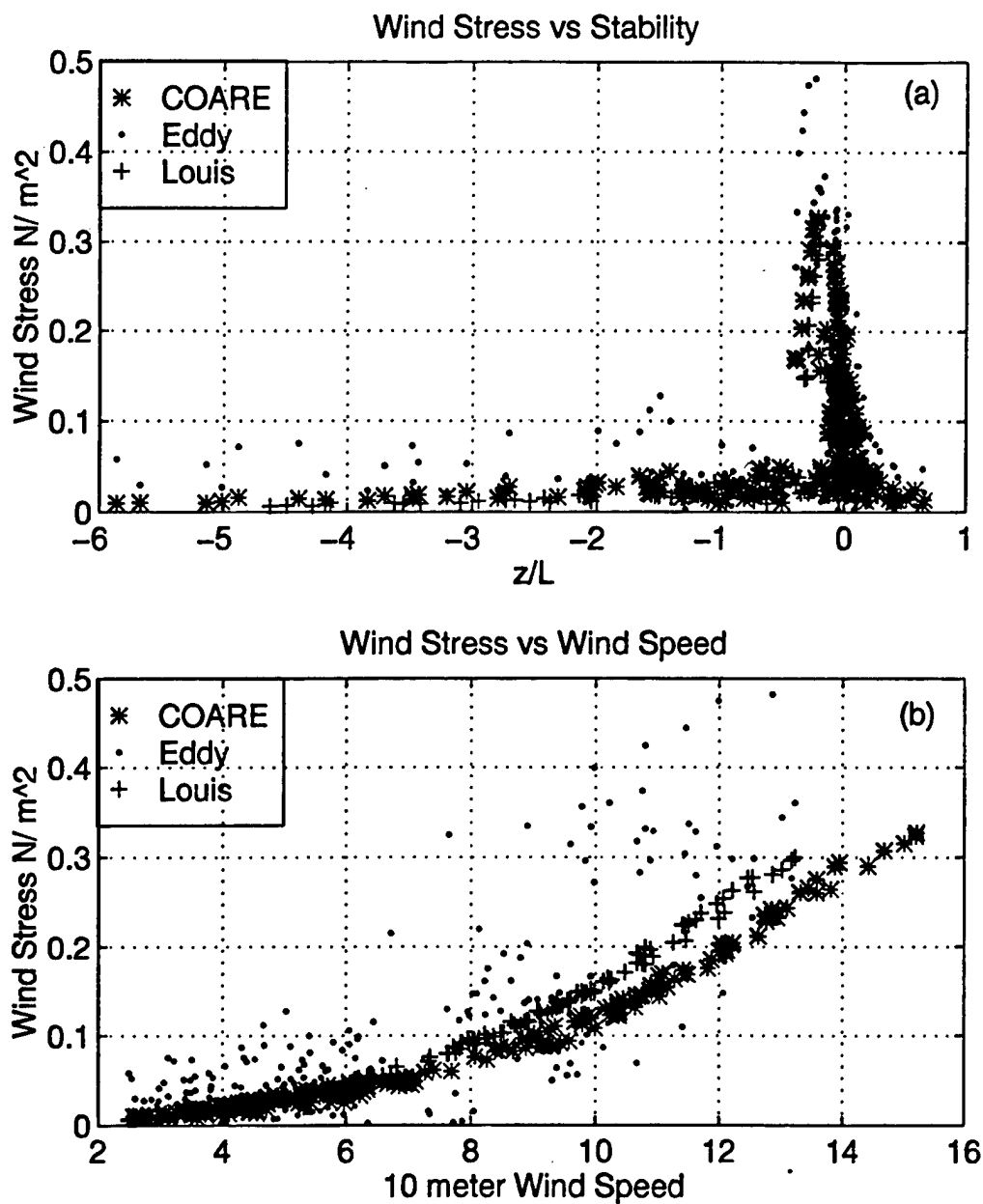
Figure 13. Variations of wind stress as a function of (a), static stability and (b), 10 m wind speed, for all analyzed flights during the ACE-1 IOP. The method used to obtain the fluxes is indicated in the legend.

Figure 14. Same as Fig. 13 except for sensible heat flux.
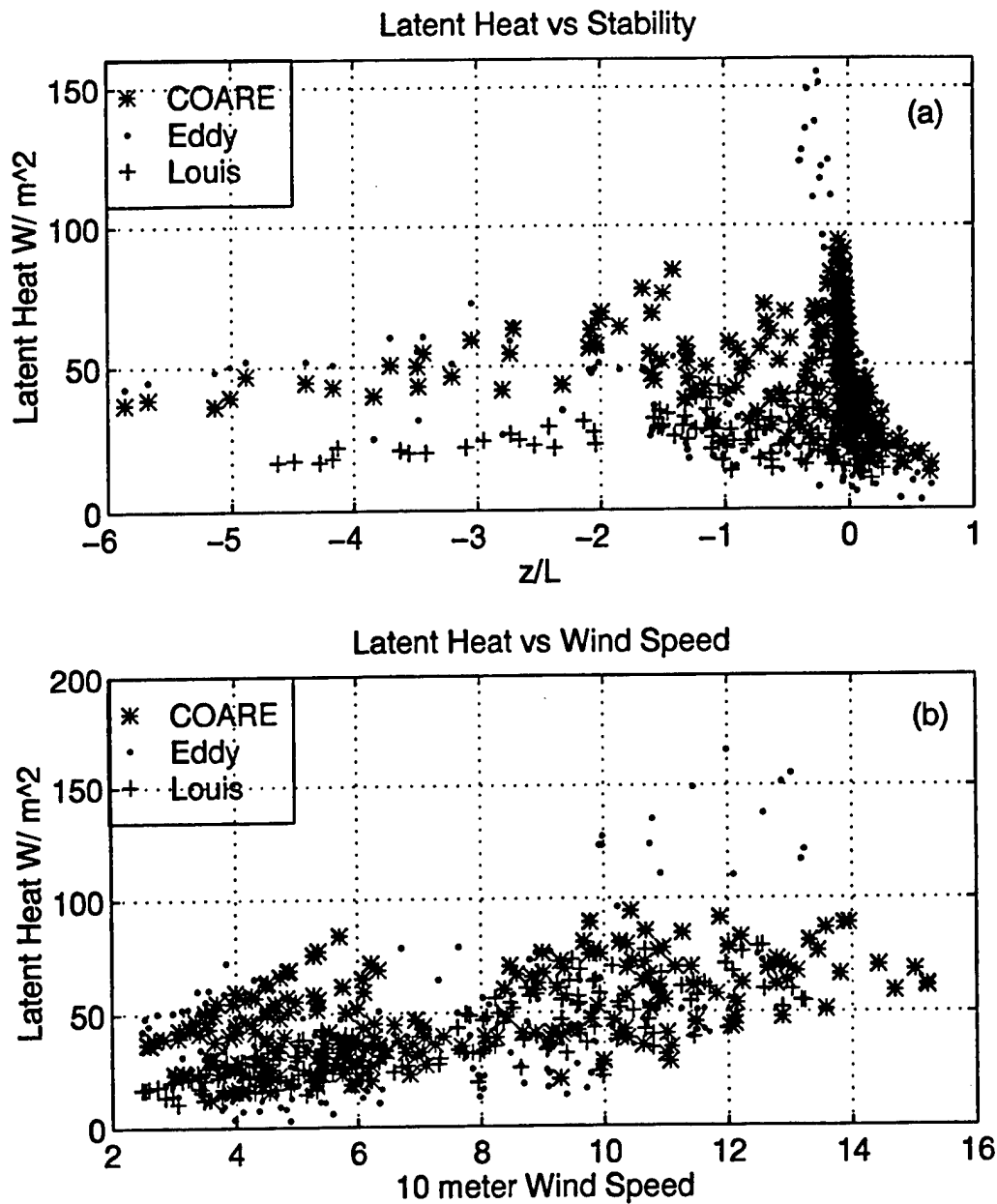
Figure 15. Same as Fig. 13 except for latent heat flux.
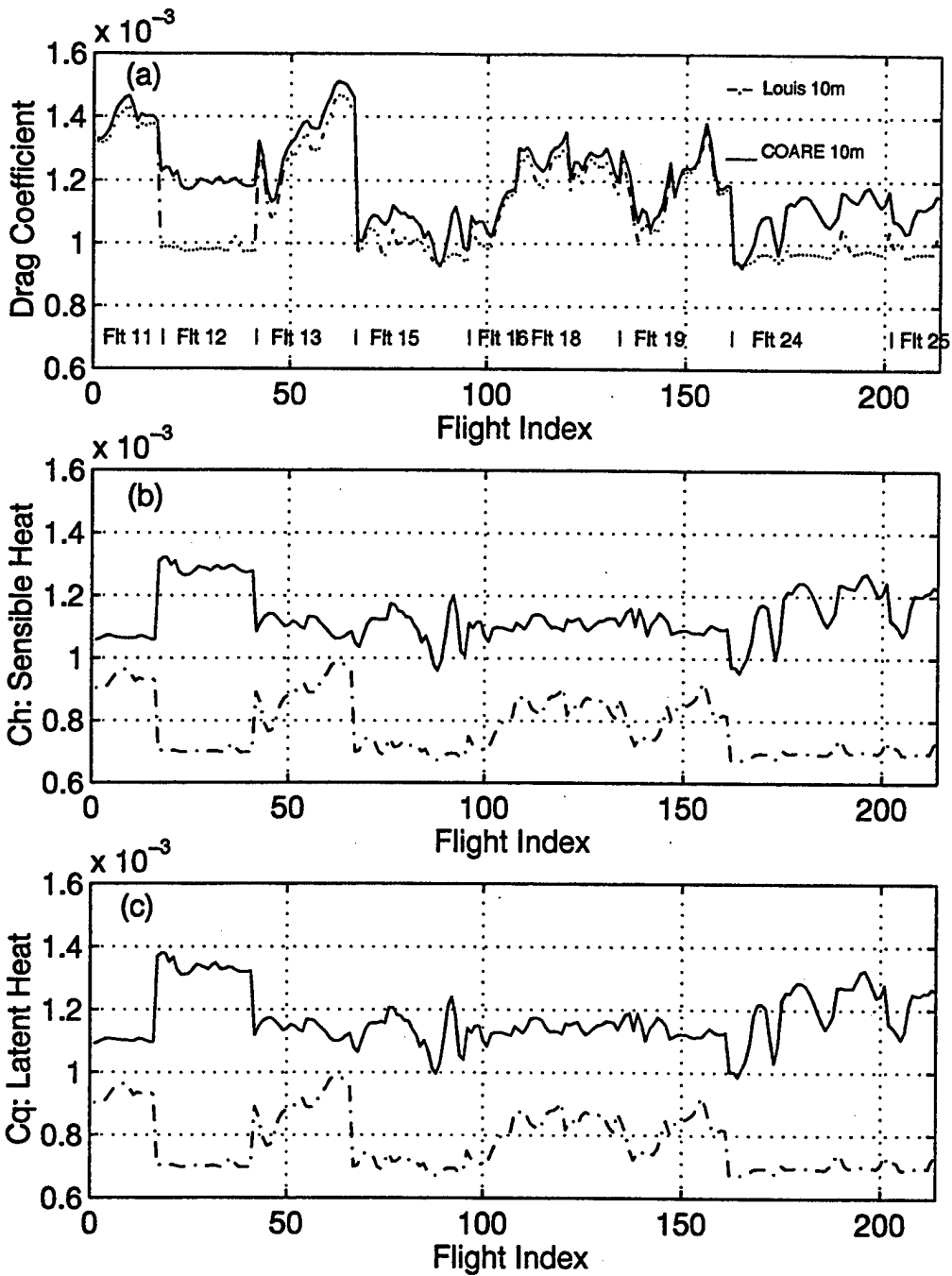
Figure 16. Bulk transfer coefficients at 10m height obtained from the Louis and COARE methods analyzed from flights during the ACE-1 IOP. Flight numbers are indicated in (a).
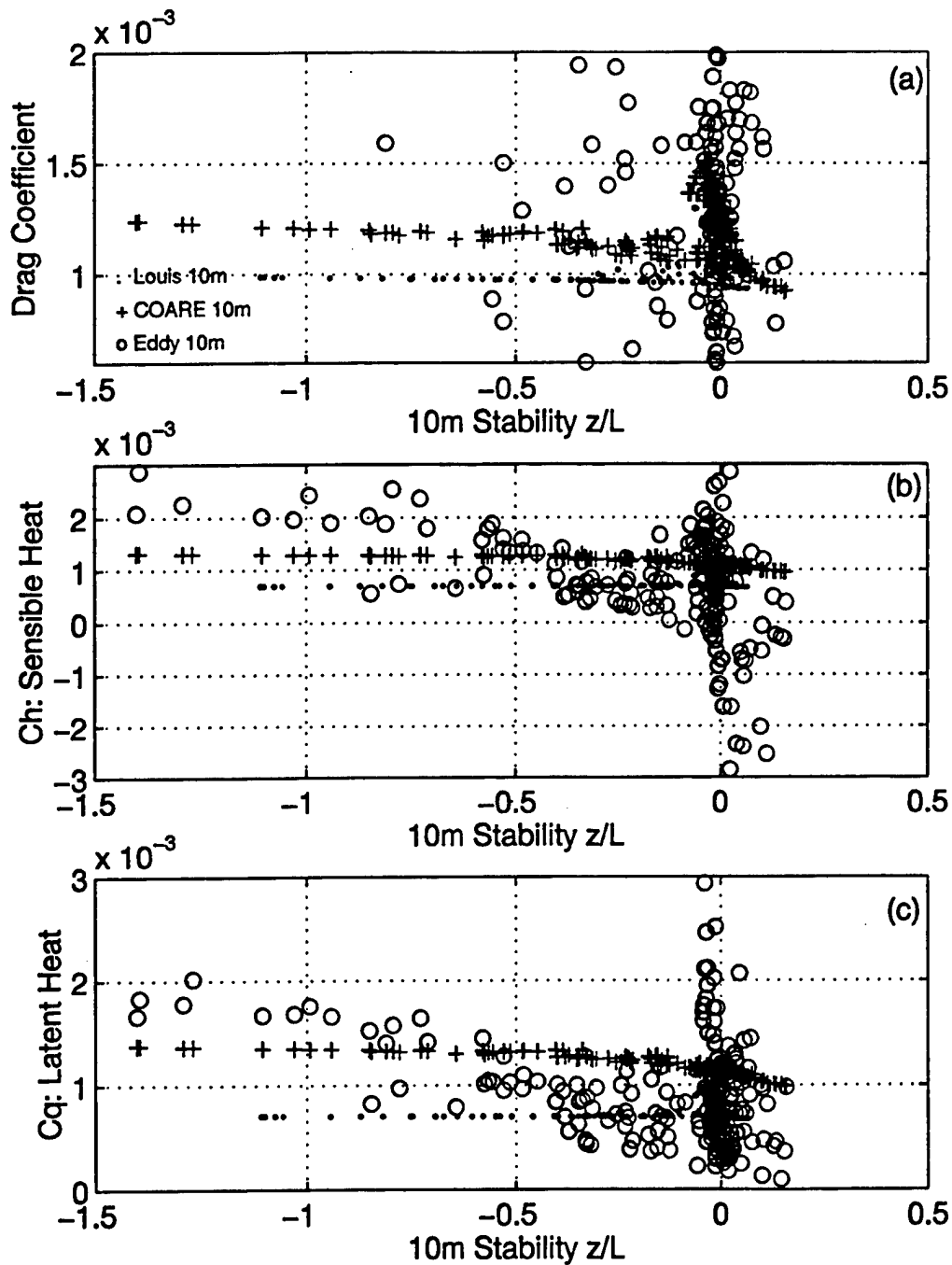
Figure 17. Bulk transfer coefficients at 10m height as a function of static stability. The method used to obtain the transfer coefficients is indicated in the legend.
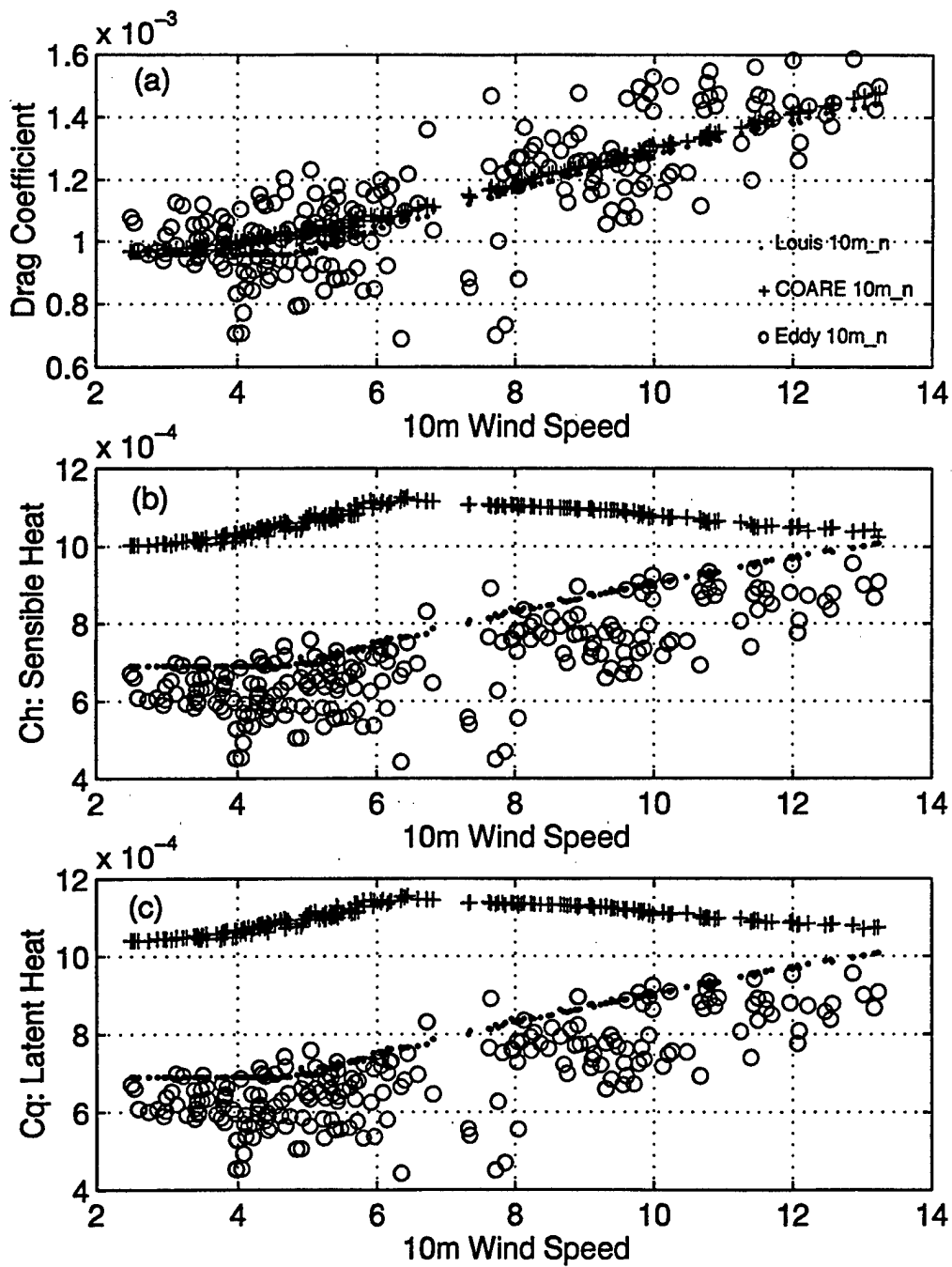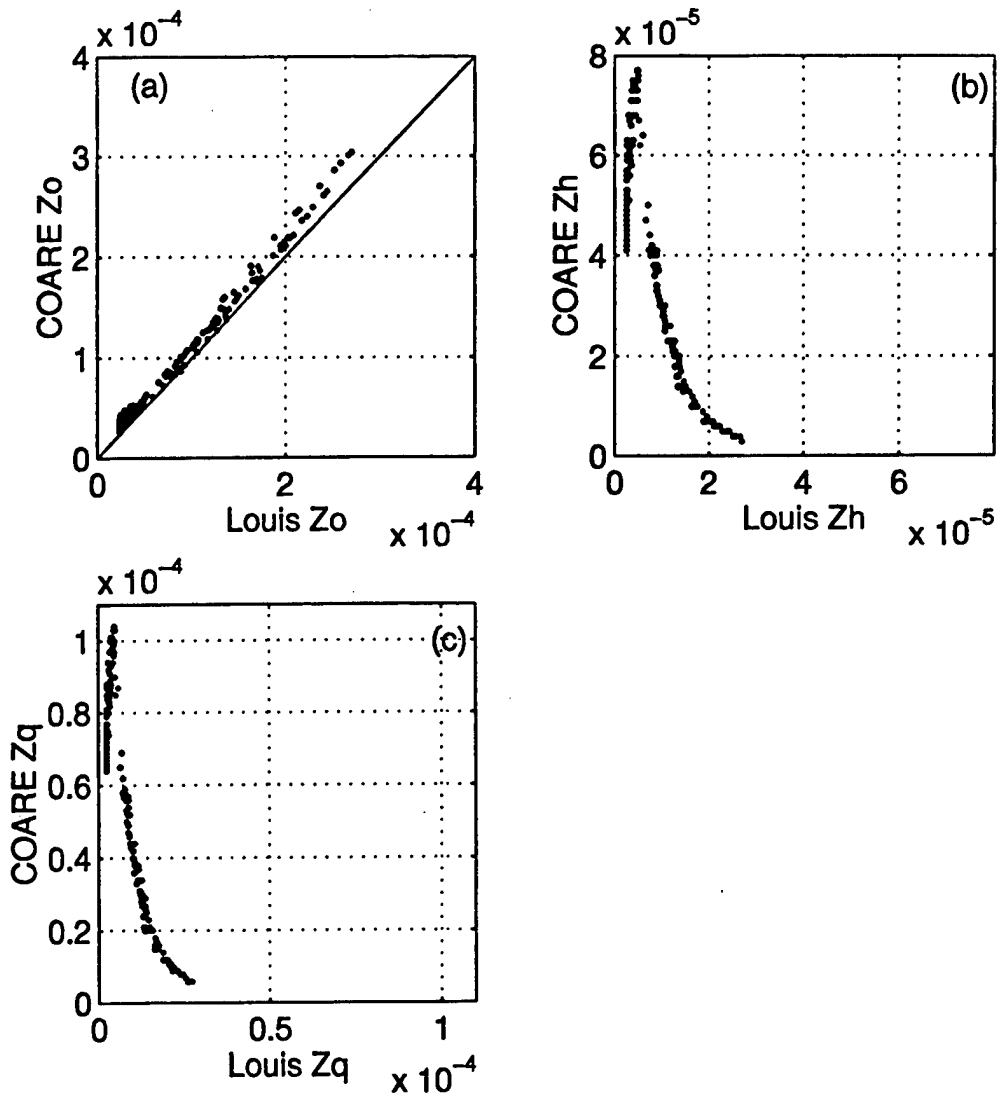
Figure 18. Neutral bulk transfer coefficients at 10m height as a function of 10m wind speed. The method used to obtain the transfer coefficients is indicated in the legend.

Figure 19. Comparison of roughness lengths for momentum
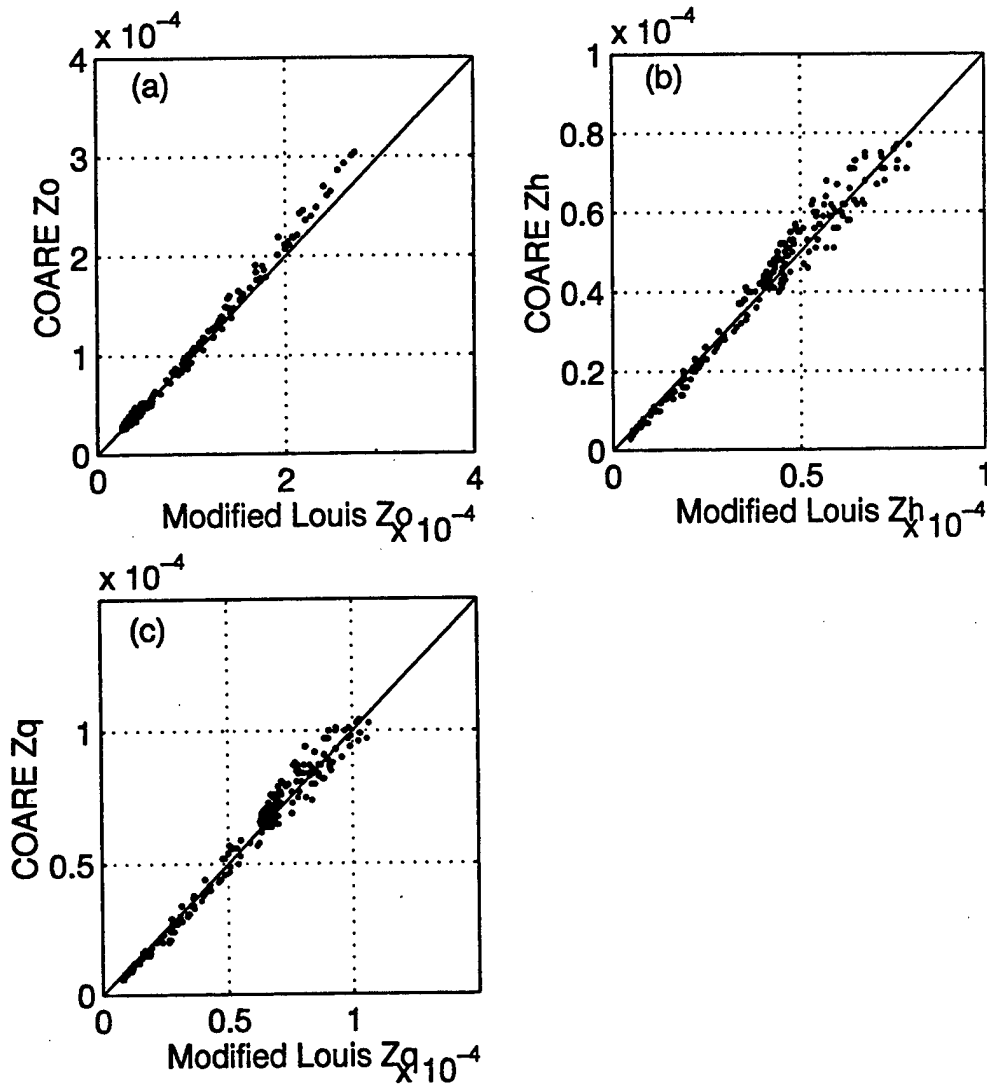(z_{0m}), heat (z_{0h}) and moisture (z_{0q}) between the Louis and
COARE algorithms.

Figure 20. Comparison of roughness lengths for momentum (z_0), heat (z_{0h}) and moisture (z_{0q}) between the Louis method modified to use the COARE parameterization and from the COARE algorithm. Differences are due to different initial estimates of u_* in the two methods.
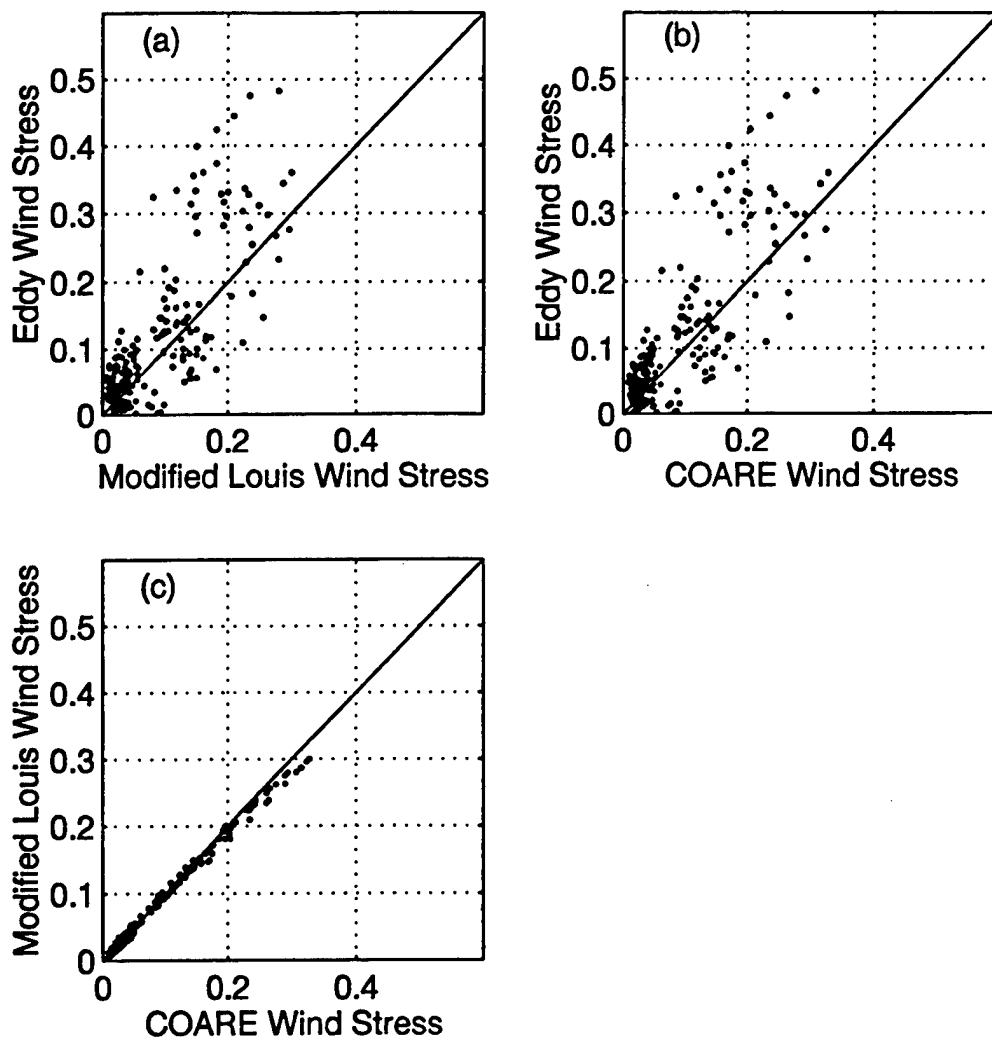
Figure 21. Comparison between the calculated wind stress (N m^{-2}) using the modified Louis method and the COARE algorithm and the observed wind stress from the eddy correlation method.
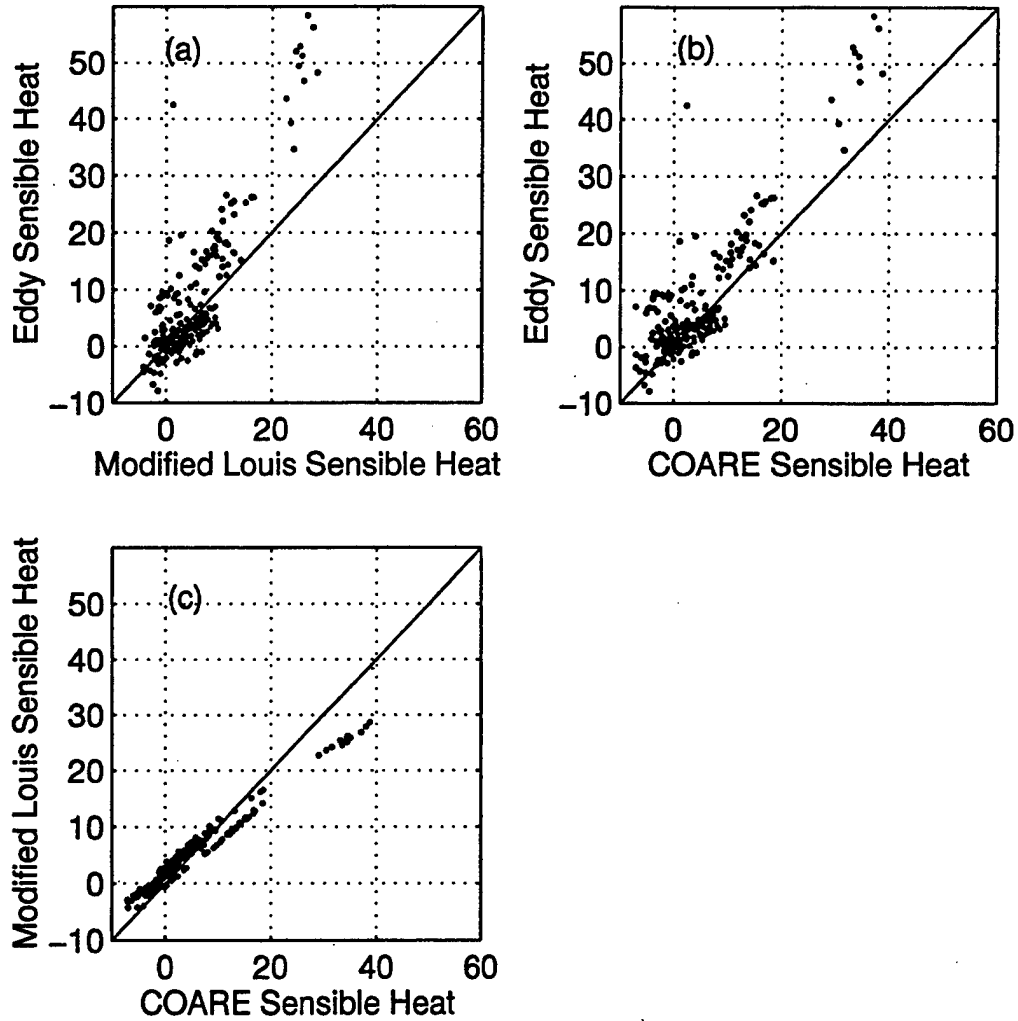
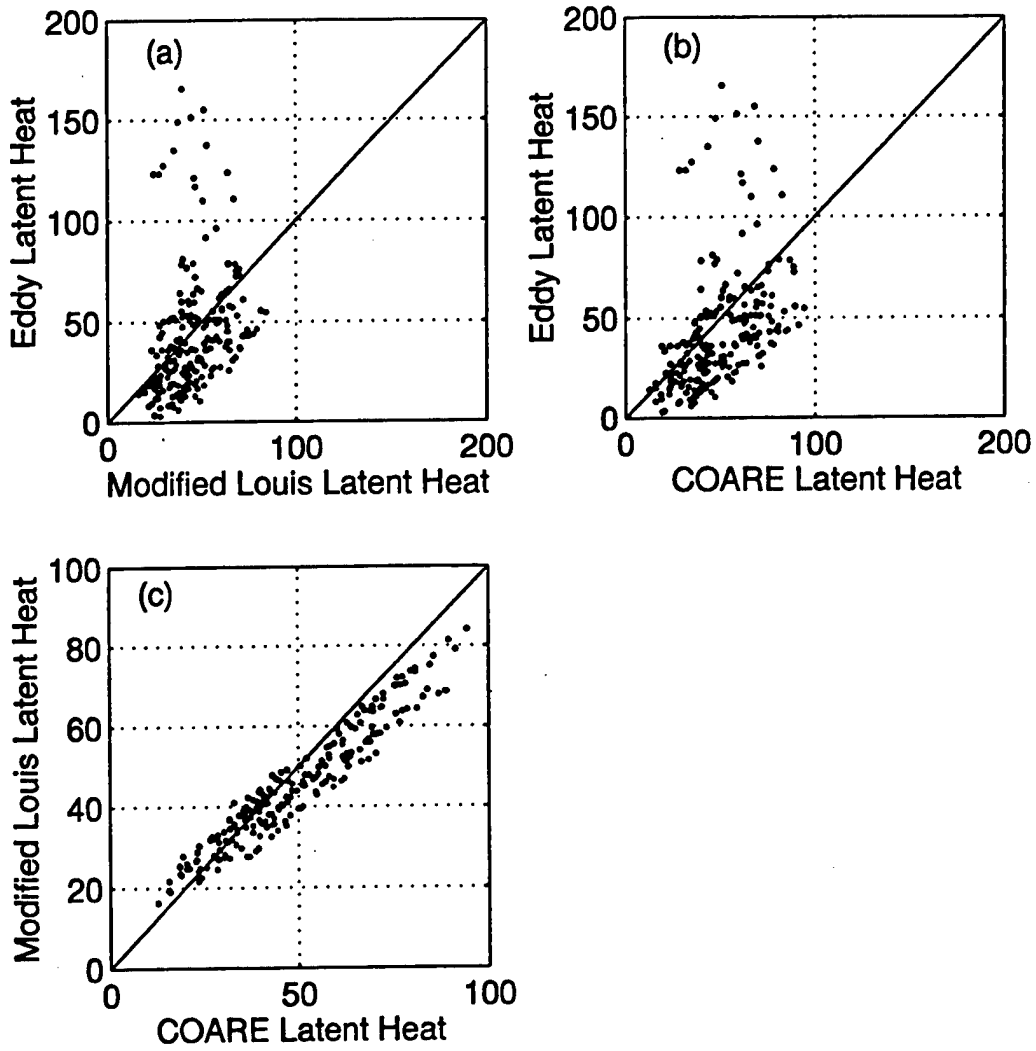Figure 22. Same as Fig. 21, except for sensible heat flux.

Figure 23. Same as Fig. 21, except for latent heat flux.

V. SUMMARY AND CONCLUSIONS

The Louis et al. (1982) flux parameterization as applied in the COAMPS model was compared to the TOGA-COARE flux algorithm using observations collected during ACE-1, 15 November 1995 to 15 December 1995 in the South Pacific Ocean southwest of Tasmania. The Louis method is computationally very compact and works well for previous forecast models. However, improvements in numerical models and the increasing effort in modelling coupled air-sea systems requires improved accuracy in the air-sea flux calculations. The TOGA-COARE flux algorithm is a state-of-the-art method incorporating several physical considerations neglected in earlier turbulent flux parameterizations. This method is specifically designed to produce more accurate flux estimates from bulk methods but is an iterative approach that is more computationally expensive. As this method is to be incorporated into the U. S. Navy's Coupled Ocean-Atmosphere Mesoscale Prediction System (COAMPS), it is desirable to evaluate its performance relative to the existing flux parameterization (Louis at al., 1982) and direct observations.

These two methods were found to be extremely sensitive to accurate sea surface temperature (SST) measurements. A detailed analysis of all available SST data was conducted in order to ensure adequate accuracy of the specified skin

73

temperature from the observations. Comparison of shipboard and satellite-derived SST estimates with the aircraft data indicated that the aircraft data had a consistent low bias. The warm-layer correction algorithms incorporated in the TOGA-COARE method were used to adjust the observed ship inlet temperatures to skin temperature for this comparison. The modeled warm layer correction based on observed radiative warming and surface turbulent fluxes was found to vary from 0.1 to 1.3 °C in the ACE-1 region. This correction was particularly sensitive to wind stress and was minimal for wind stresses above 0.03 N m^{-2}. The resultant adjustment of the aircraft observations of sea surface temperatures was found to greatly improve the resultant fluxes.

The two bulk methods showed close agreement with each other and with eddy correlation measurements of the actual fluxes for momentum flux. For latent and sensible heat flux, the two methods showed good agreement in low flux regimes but both methods underestimated the flux for values above 20 W m^{-2} for sensible heat flux and 70 W m^{-2} for latent heat flux.

The high heat and moisture flux cases can be separated into two regimes, cases with wind speeds above 10 m s^{-1}, which were also characterized by near neutral stability, and cases with low wind speeds, which were also highly convective. Calculation of the required transfer

coefficients from the directly observed fluxes indicates that the transfer coefficients in the bulk methods do not increase rapidly enough for z/L values less than -0.5. In the high wind regime, the transfer coefficients are seen to be very sensitive to static stability.

In general, the COARE method was found to be better than the Louis method in estimating the sensible heat flux while the Louis method was superior for latent heat flux. The observed decrease in latent and sensible heat transfer coefficients with wind speed in the COARE model was similar to the decrease in heat and moisture roughness lengths with u_* in the COARE parameterization. The Louis method was modified to match the more sophisticated COARE parameterization for momentum, thermal, and moisture roughness lengths. Little improvement was found for estimates of wind stress, which is expected since the additional term in the COARE model accounts for smooth flow regimes which were not observed in this study. Sensible heat flux estimates were observed to improve slightly in the modified Louis method, especially at higher flux levels, but modifying the thermal roughness length in the Louis method did not improve the sensible heat flux estimates in stable conditions. The modified Louis method was found to overestimate the latent heat flux in the same manner as the COARE algorithm which indicates that the parameterization

for latent heat roughness length in the COARE algorithm requires further study.

The observations and analysis in this study indicate that bulk flux parameterizations seem to break down in high wind and highly convective conditions. This is not surprising as the field studies and theoretical treatments used in developing Monin-Obukhov similarity theory are often based on mean synoptic environments and surface layer profiles. Accurate estimates of heat and moisture flux in these regimes are particularly sensitive to the correct formulation for heat and moisture roughness lengths and our observations indicate that moisture roughness length in particular requires further study. In high wind conditions, static stability approaches near neutral conditions, however heat and moisture fluxes are still quite strong, and an accurate estimate of these fluxes is very sensitive to small variations in the stability parameter (z/L). This in turn requires very accurate specification of the air-sea temperature contrast, which requires better SST measurements than are currently available in operational models.

LIST OF REFERENCES

Bates, T. S., B. J. Huebert, J. L. Gras, F. B. Griffiths, and P. A. Durkee, 1998: International Global Atmospheric Chemistry (IGAC) Project's first Aerosol Characterization Experiment (ACE 1): Overview. *J. Geophys. Res.*, **103**, 16,297-16,318.

Beljaars, A.C.M., and A. A. M. Holtslag, 1991: Flux parameterization over land surfaces for atmospheric models. *J. Appl. Met.*, **30**, 327-341.

Black, P. G. and G. J. Holland, 1995: The boundary layer of Tropical Cyclone Kerry (1979). *Mon. Wea. Rev.*, **123**, 2007-2028.

Charnock, H., 1955: Wind stress over a water surface. *Q. J. R. Meteorol. Soc.*, **81**, 639.

Chou, S.-H., 1993: A comparison of airborne eddy correlation and bulk aerodynamic methods for ocean-air turbulent fluxes during cold-air outbreaks. *Boundary-Layer Meteorol.*, **64**, 75-100.

DeCosmo, J. K., B. Katsaros, S. D. Smith, R. J. Anderson, W. A. Oost, K. Bumke, and H. Chadwick, 1996: Air-Sea exchange of water vapor and sensible heat: The Humidity Exchange Over the Sea (HEXOS) results. *J. Geophys. Res.*, **101**, C5, 12001-12016.

Delage. Y., 1997: Parameterising sub-grid scale vertical transport in atmospheric models under statically stable conditions. *Boundary-Layer Meteorol.*, **82**, 23-48.

Fairall, C. W., E. F. Bradley, J. S. Godfrey, G. A. Wick, J. B. Edson, and G. S. Young, 1996a: Cool-skin and warm-layer effects on sea surface temperature. *J. Geophys. Res.*, **101**, C1, 1295-1308.

Fairall, C. W., E. F. Bradley, D. P. Rogers, J. B. Edson, and G. S. Young, 1996b: Bulk parameterization of air-sea fluxes for Tropical Ocean-Global Atmosphere Coupled-Ocean Atmosphere Response Experiment. *J. Geophys. Res.*, **101**, C2, 3747-3764.

Garratt, J. R., G. D. Hess, W. L. Physick, and P. Bougeault, 1996: The atmospheric boundary layer - advances in knowledge and application. *Boundary-Layer Meteorol.*, **78**, 9-37.

Griffiths, F. B., T. S. Bates, P. K. Quinn, L. A. Clementson, and J. S. Parslow, 1998: The oceanographic context of the First Aerosol Characterization Experiment (ACE-1): A physical, chemical, and biological overview. Submitted to *J. Geophys. Res.*

Guilloteau, E., 1998: Optimize computation of transfer coefficients in surface layer with different momentum and heat roughness lengths. *Boundary-Layer Meteorol.*, **87**, 147-160.

Hainsworth, A. H. W., A. L. Dick, and J. L. Gras, 1998:Climatic context of the first Aerosol Characterization Experiment (ACE 1): A meteorological and chemical overview. *J. Geophys. Res.*, **103**, 16,319-16,340.

Hodur, R. M., 1997 : The Naval Research Laboratory's Coupled Ocean/ Atmosphere Mesoscale Prediction System (COAMPS). *Mon. Wea. Rev.*, **125**, 1414- 1430.

Holtslag, A. A. M., and A. C. M. Beljaars, 1989: Surface flux parameterization schemes: developments and experiences at KNMI. *Parameterization of fluxes over land surfaces,* Workshop Proceedings, October 1988, ECMWF, Reading, England, 121-147. [Also KNMI Sci. Rep., 88-106, 1988].

Kidder, S. Q. and T. H. Vonder Haar, 1995: Satellite meteorology: An introduction, Academic Press, 466 pp.

Launianen, J., 1995: Derivation of the relationship between the Obukhov stability parameter and the bulk Richardson number for flux-profile studies. *Boundary-Layer Meteorol.*, **76**, 165-179.

Liu, W. T., K. B. Katsaros, and J. A. Businger, 1979: Bulk parameterization of air-sea exchanges of heat and water vapor, including the molecular constraints at interface. *J. Atmos. Sci.*, **36**, 1722-1735.

Lo, A. K-F., 1996: On the role of roughness lengths in flux parameterizations of boundary-layer models. *Boundary-Layer Meteorol.*, **80**, 403-413.

Louis, J-F. 1979: A parametric model of vertical eddy fluxes in the atmosphere. *Boundary-Layer Meteorol.*, **17**, 187-202.

Louis, J-F., M. Tiedtle, and J. F. Gelyn, 1982: A short history of the operational PBL-parameterization at ECMWF.

Workshop on boundary layer parameterization, November 1981, ECMWF, Reading, England, 59-79.

McAvaney, B. J. and G. D. Hess, 1996: The revised surface fluxes parameterisation in BMRC: Formulation. *Bureau of Meteorology Research Centre Research Report No. 56,* May 1996, BMRC, Melbourne, Australia, 1-27.

NCAR, 1995: RAF sensor summaries. [Available from Research Aviation Facility, Atmospheric Technology Division, NCAR, Bolder, CO].

Pielke, R. A., W. R. Cotton, R. L. Walko, C. J. Tremback, W. A. Lyons, L. D. Grasso, M. E. Nicholls, M. D. Moran, D. A. Wesley, T. J. Lee, and J. H. Copeland, 1992: A comprehensive meteorological modeling system - RAMS. *Meteorol. Atmos. Phys.,* **49,** 69-91.

Price, J. F., R. A. Weller, and R. Pinkel, 1986:Diurnal cycling: Observations and models of the upper ocean response to diurnal heating, cooling, and wind mixing. *J. Geophys. Res.,* **91,** 8411-8427.

Smith, S. D. 1980: Wind stress and heat flux over the ocean in gale force winds. *J. Phys. Oceanogr.,* **10,** 709-726.

Stull, R. B., 1988: *An Introduction to Boundary Layer Meteorology,* Kluwer Academic Publishers, Dordrecht, The Netherlands, 670 pp.

Uno, I., X-M. Cai, and D. G. Steyn, 1995: A simple extension of the Louis method for rough surface layer modelling. *Boundary-Layer Meteorol.,* **76,** 395-409.

Van den Hurk, B. J. J. M., and A. A. M. Holtslag, 1997: On the bulk parameterization of surface fluxes for various conditions and parameter ranges. *Boundary-Layer Meteorol.,* **82,** 119-134.

Wang, Q., K. Suhre, P. Krummel, S. Siems, L. Pan, T. S. Bates, J. E. Johnson, D. H. Lenschow, B. J. Heubert, G. L. Kok, R. D. Schillawski, A. S. H. Prevot, and S, Businger, 1998a: Characteristics of the marine boundary layers during two Lagrangian measurement periods, Part I: General conditions and mean characteristics. Submitted to *J. Geophys. Res.*

Wang, Q., K. Suhre, P. Krummel, S. Siems, L. Pan, T. S. Bates, J. E. Johnson, D. H. Lenschow, B. J. Heubert, G. L. Kok, R. D. Schillawski, A. S. H. Prevot, and S, Businger, 1998b: Characteristics of the marine boundary layers during two Lagrangian measurement periods, Part II: Turbulence structure. Submitted to *J. Geophys. Res.*

INITIAL DISTRIBUTION LIST